

We are IntechOpen, the world's leading publisher of Open Access books Built by scientists, for scientists

6,900

Open access books available

186,000

International authors and editors

200M

Downloads

Our authors are among the

154

Countries delivered to

TOP 1%

most cited scientists

12.2%

Contributors from top 500 universities



WEB OF SCIENCE™

Selection of our books indexed in the Book Citation Index
in Web of Science™ Core Collection (BKCI)

Interested in publishing with us?
Contact book.department@intechopen.com

Numbers displayed above are based on latest data collected.
For more information visit www.intechopen.com



Carbon Nanotube-Based Polymer Composites: Synthesis, Properties and Applications

Waseem Khan, Rahul Sharma and Parveen Saini

Additional information is available at the end of the chapter

<http://dx.doi.org/10.5772/62497>

Abstract

The present chapter covers the designing, development, properties and applications of carbon nanotube-loaded polymer composites. The first section will provide a brief overview of carbon nanotubes (CNTs), their synthesis, properties and functionalization routes. The second section will shed light on the CNT/polymer composites, their types, synthesis routes and characterization. The last section will illustrate the various applications of CNT/polymer composites; important properties, parameters and performance indices backed by comprehensive literature account of the same. The chapter concludes with the current challenges and future aspects.

Keywords: carbon nanotubes (CNTs), conducting polymer, nanocomposites, EMI shielding and supercapacitors, thermoelectrics and photovoltaics

1. Introduction

Since their discovery in 1991 by Prof. Iijima [1], carbon nanotubes (CNTs) have been a subject of global research focus, owing to their remarkable properties and related fascinating applications [2–14]. It is worth mentioning here that except in few cases, CNTs cannot be used in its bulk form (i.e. powder, aligned stacks, films/papers, etc.) due to the poor translation of outstanding inherent properties of individual CNTs into its macroscopic forms. Therefore, the most applications of CNTs involve their strategic combination with other materials in the form of alloys, blends, composites or hybrid materials [15–23]. In particular, idea of incorporating CNTs as filler inside various polymer-based matrices (e.g. conventional polymers such as thermoplastics, thermosets or elastomers as well as conjugated polymers) to form CNTs/polymer nanocomposites [13, 14] has revolutionized the materials science and technology. This

facilitates the synergistic combination of flexibility, low density and facile processing of conventional polymers with outstanding mechanical, thermal and electrical properties of CNTs, or even introduction of additional electrical/thermal/electromagnetic attributes, thereby extending their field of applicability. In this context, attempts have also been made to form CNTs-filled conjugated polymer (CP) composites, to club the specialties of CNTs with good electroactivity, interesting doping-dependent properties and solution processability of CPs. Therefore, inspired by their scientific and technological potential, over two decades, a lot of research work has been done on CNTs/polymer nanocomposite [19–21, 24–28] and the area is still growing stronger.

2. Carbon nanotubes

2.1. Structure of carbon nanotubes

The electronic configuration of carbon atom is $1s^2 2s^2 2p^2$ indicating that it has two strongly bound electrons in the 1s orbital and four relatively weakly bound electrons in 2s and 2p orbitals known as valence electrons. The small energy difference between 2s and 2p levels allows the carbon atom to exist in several hybridization states; sp , sp^2 and sp^3 in different materials (**Figure 1**).

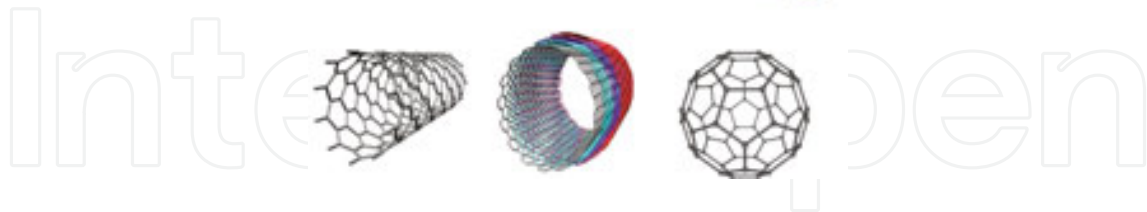
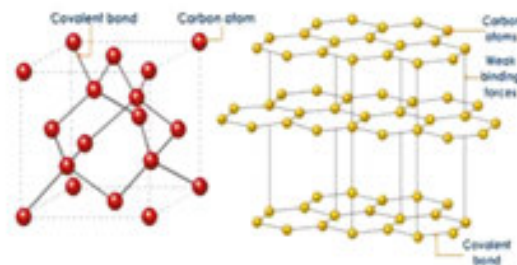


Figure 1. Schematic diagrams of diamond, graphite, fullerene single-wall carbon nanotube (SWCNT) and multi-wall carbon nanotube (MWCNT).

The hybridization flexibility enables the atomic orbitals of carbon to arrange themselves in structures of different dimensionalities ranging from diamond (3D), graphite (2D), carbon nanotubes (1D) and fullerene (0D). CNTs are hollow cylinders of graphene with extraordinary electronic and mechanical properties. They exist in two varieties viz. CNTs composed of a single graphene sheet called single-wall carbon nanotubes (SWCNTs) and an array of coaxial nanotubes known as multiwall carbon nanotubes (MWCNTs) [29, 30].

In the honeycomb lattice (**Figure 2**), the vector C_h is called chiral vector, while T is called the translational vector. The rectangle generated by the chiral vector C_h and the translational vector T is the unit cell of the SWCNT in real space. The chiral angle is defined as the angle between the chiral vector C_h and the unit vector a_1 . The chiral vector can be expressed in terms of the unit vectors a_1 and a_2 by means of integers (n, m) (which are called chiral indices):

$$C_h = n a_1 + m a_2$$

The wrapping of graphene sheet is governed by the different orientations of the chiral vector leading to the different CNT geometries. When the chiral indices are equal ($n = m$), the SWCNT is called armchair, and the chiral angle is 30° . If one of the chiral index is zero ($n, 0$) or $(0, m)$, the SWCNT is named zig-zag, and in this case, the chiral angle is 0° (achiral nanotubes). In the other cases ($n \neq m$), the nanotube is called chiral and its chiral angle is $0^\circ < \theta < 30^\circ$.

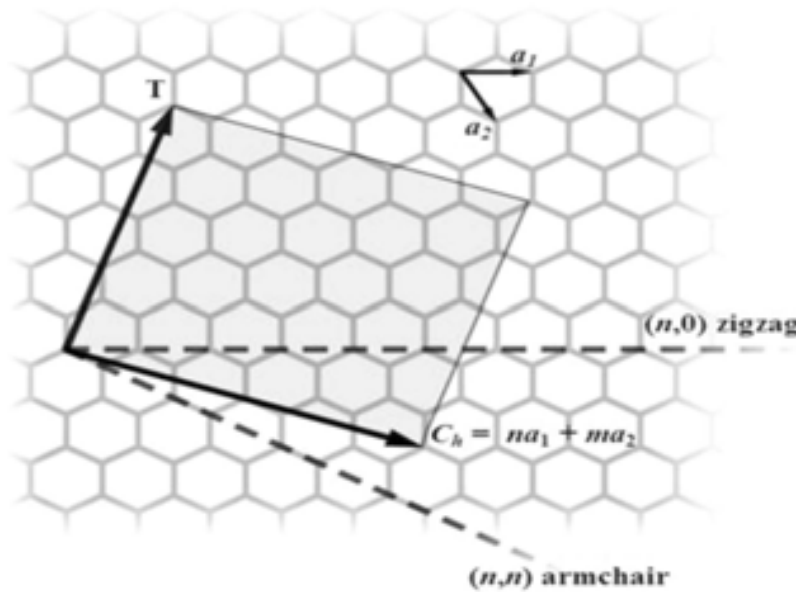


Figure 2. Chiral vector C_h and chiral angle θ definition for a nanotube on graphene sheet. a_1 and a_2 are the unit cell vectors of the two-dimensional hexagonal graphene sheet.

The expressions for the main parameters of a tube as a function of the chiral indices (n, m) are 29, 30:

$$\text{nanotube diameter } D = a\sqrt{(n^2 + m^2 + nm)}$$

$$\text{with, } a = a_{C-C}\sqrt{3} = 1.44 \text{ \AA}$$

$$\text{Chiral angle } \theta, \cos \theta = \frac{(2n + m)}{2\sqrt{(n^2 + m^2 + nm)}}$$

In addition to above structural details, important physical attributes of CNTs that decide their properties are described below:

2.1.1. Length, diameter and aspect ratio

The actual length of CNTs is expected to influence their physical status as well as acquired configuration inside polymer matrix. In general, long-length CNTs show a flexible fibre-like character with tube buckling and entangled configuration. Therefore, its processing inside polymer matrix is a bit difficult in terms of de-entanglements. The long length ensures lower electrical percolation threshold, good mechanical properties due to the large-distance stress transfer and crack propagation prevention ability. In contrast, the short-length CNTs display rod-like character, provide more stiffness (compared to long-length CNTs of similar loading) to composite, and has relatively large percolation threshold, inferior stress transfer, poor crack countering property, low tensile/flexural strength and elongation of composites. However, it can be easily aligned and tends to show better interfacial polarization. Like the length of CNTs, diameters also affect the properties, for example SWCNTs, large diameter offers large interfacial surface area per unit length but less stiffness. Similarly, for MWCNTs, large diameter means more number of cylindrical graphitic tubular shells (i.e. thick walls), which tends to improve inherent mechanical properties of tubes, its stiffness, electrical properties and ability to undergo functionalization without much harm in tube's properties. Another important parameter is aspect ratio (i.e. length/diameter ratio), which affects the properties via interplay of length and diameter. However, it could be bit elusive and care has to be taken while talking about aspect ratio because a short-length and small-diameter CNT can have same aspect ratio as a long-length and large-diameter CNT, but their properties and translated effect on composites may be altogether different. Nevertheless, CNTs are widely used as very small, high aspect ratio conductive additives for plastics of all types. The high aspect ratio (up 1000 or more) gives CNTs an edge over other conductive fillers (e.g. carbon black, chopped carbon fibre, carbon nanofibres, stainless steel fibres or whiskers) as a lower loading of CNTs is needed to achieve the same electrical conductivity. This low loading preserves polymer resin's toughness, especially at low temperatures and maintains other key properties of the matrix resin.

2.1.2. Defects

A perfect single-wall CNT is only a theoretical construction and even perfect hexagonal sp^2 structure possesses different types of defects. Generally, a defective site has a high reactivity meaning that at those points, the chemical reactions are favoured. A simple example of a defect is the presence of non-hexagonal-shaped carbon rings such as a pentagon and heptagon pair (also known as Stone/Wales defect or 5/7 defect) [31–34]. They are localized mainly at tube ends and near tube bending locations. A Stone/Wales defect has very significant role to play in the modification of density of states of nanotubes which has implications for possible nanodevice applications [35–39]. Defects are very important because they can modify the electronic properties of the nanotubes thereby influencing their applications. The distribution of the 5/7 defects in the capping of the CNTs can induce the presence of new localized states

in the valence and/or the conduction band, and so to modify the field emission properties [40, 41]. The introduction of a 5/7 defect in the hexagonal structure can induce a local deformation of the diameter of the tube, a change of the chirality or the formation of a CNT intramolecular junction. The defects can also be present along the sidewall, and after acid treatment, it is possible to open nanotube ends and attach chemical functional groups facilitating the interaction of CNTs with other moieties. In addition to being important for the potential applications of nanotubes, defects also play a key role in the functionalization process.

2.2. Synthesis methods of carbon nanotubes

2.2.1. Arc discharge method

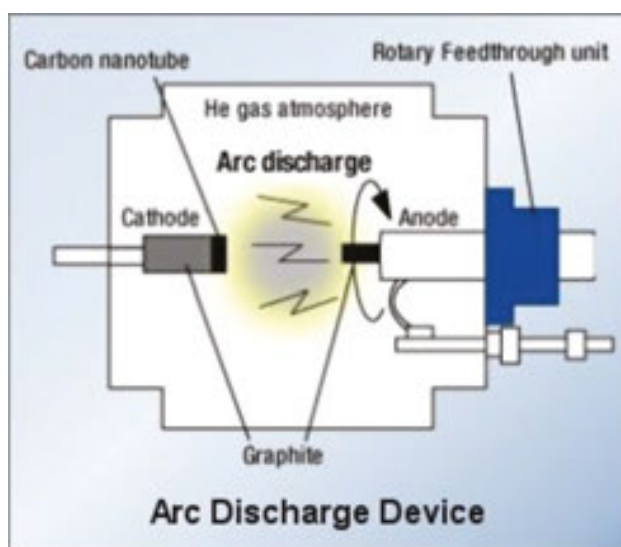


Figure 3. Schematic diagram of Arc-discharge setup.

The carbon arc-discharge method was first brought to light by Krätschmer et al. [42] who utilized it to achieve the production of fullerenes in macroscopic quantities. As mentioned in the introduction of this chapter, Iijima discovered the catalyst-free formation of multiwall carbon nanotubes (MWCNTs), while investigating the other carbon nanostructures formed along with the fullerenes and more particularly, the solid carbon deposit forming onto the cathode. **Figure 3** shows the schematic diagram of the arc-discharge method. This method creates CNTs through arc-induced vapourization of two carbon rods placed end to end, separated by approximately 1 mm, in an enclosure usually filled with inert gas (argon or helium) at low pressure. A direct current of 50–100 A, driven by a potential difference of approximately 20 V, creates a high-temperature discharge between the two electrodes, vapourizes the surface of one of the carbon electrodes, and forms a small rod-shaped deposit on the other electrode. This technique produces a complex mixture of components including non-tubular forms of the carbon such as nanoparticles, fullerene-like structures including C_{60} , multiwall shells, amorphous carbon, etc. [43–45]. Therefore, this requires further purification to separate the CNTs from the soot and the residual catalytic metals present in the crude

product. In this technique, the high yield production of CNTs depends on the uniformity of the plasma arc, and the temperature of the deposit forming on the carbon electrode.

2.2.2. Laser ablation method

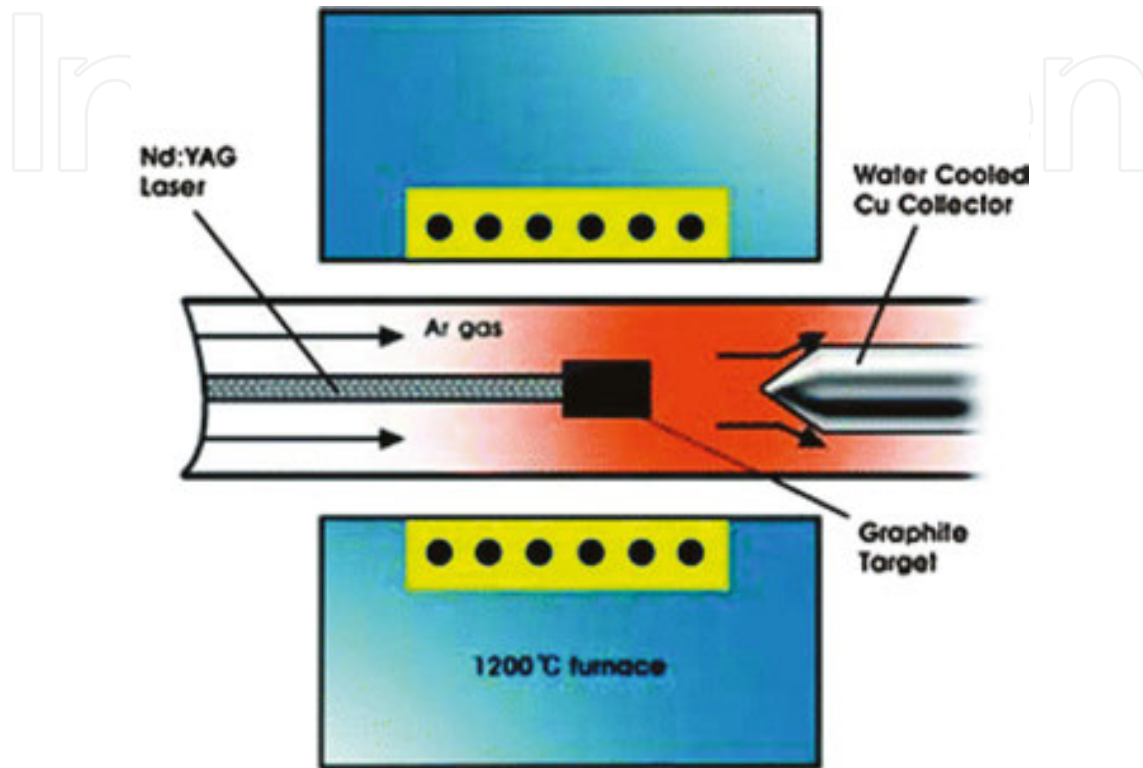


Figure 4. Schematic diagram of laser ablation setup.

The laser ablation technique was used successfully to synthesize fullerene for the first time in 1985 by Kroto et al. [46]. However, the synthesis of carbon nanotubes by this technique could be possible only 10 years later in 1995 by Guo et al. [47].

Figure 4 shows the schematic diagram of laser ablation method. Samples are prepared by laser vapourization of graphite rods with a 50:50 catalyst mixture of cobalt and nickel at 1200°C in flowing argon, followed by heat treatment in a vacuum at 1000°C to remove the C₆₀ and other fullerenes. The target is vapourized more uniformly by a second laser pulse. The use of two successive laser pulses minimizes the amount of carbon deposited as soot. The second laser pulse breaks up the larger particles ablated by the first one and feeds them into the growing nanotube structure.

The material produced by this method appears as a 'mat' of ropes, 10–20 nm in diameter and up to 100 µm or more in length. Each rope primarily consists of a bundle of SWCNTs, aligned along a common axis. It is possible to vary the average nanotube diameter and size distribution by varying the growth temperature, the catalyst composition and other process parameters.

Both these solid carbon source-based synthesis methods have some drawbacks. One issue is the scaling up of the process to the industrial level. Secondly, the synthesized CNTs have impurities of metal catalyst particles and unwanted carbon forms such as fullerenes, amorphous carbon, multiwall shells, single-wall nanocapsule and need further purification.

2.2.3. Chemical vapour deposition method

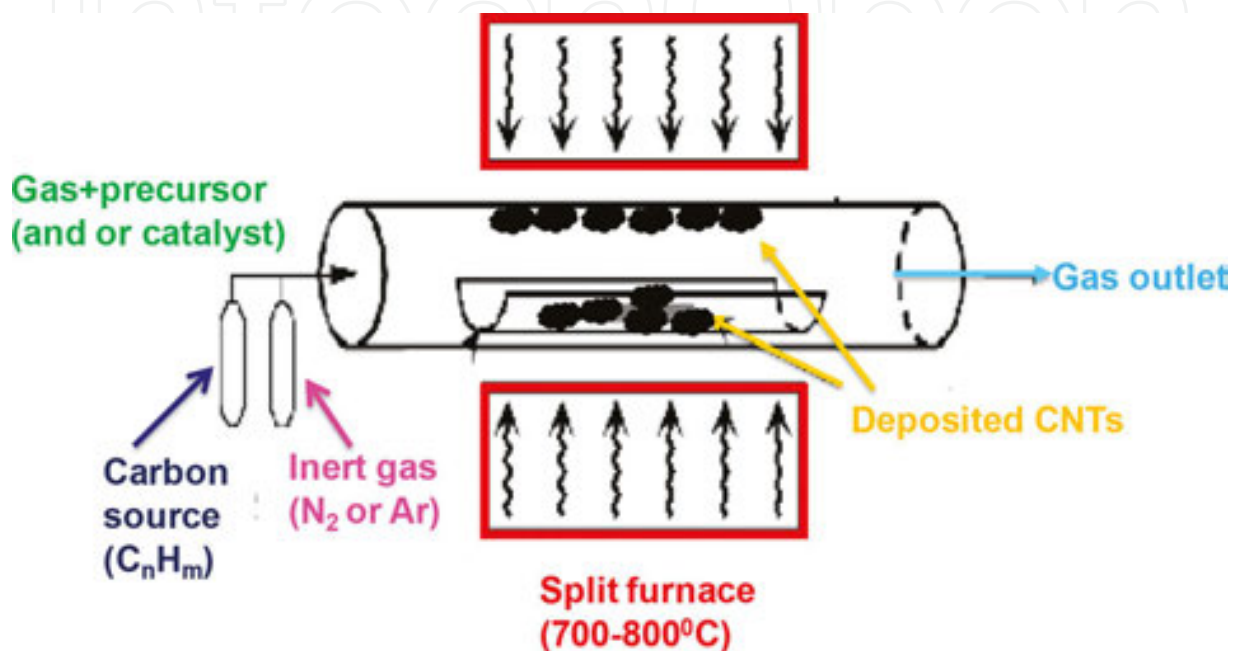


Figure 5. Schematic diagram of chemical vapour deposition setup.

Chemical vapour deposition (CVD) of gaseous carbon source (hydrocarbons, CO) over a metal catalyst is a classical method that has been used to produce various carbon materials such as carbon fibres and filaments for a long time [48]. However, CVD technique was first reported to produce MWCNTs by Endo and his research group [49]. Three years later, Dai in Smalley's group successfully adapted CO-based CVD to produce SWCNTs [50].

Figure 5 shows the schematic diagram of CVD method. In this technique, a carbon source is taken in the gas phase and an energy source such as plasma or a resistively heated coil is employed to transfer energy to a gaseous carbon molecule. The CVD technique uses hydrocarbons such as methane, carbon monoxide or acetylene as carbon source. During CVD, a substrate covered with metal catalysts (such as nickel, cobalt, iron or their combination) is heated to approximately 700°C. The growth starts after two gases are passed through the chamber, that is hydrocarbon gas and the other a carrier gas such as nitrogen, hydrogen or argon. The advantages of the CVD process are low power input, low-temperature range, relatively high purity and most importantly, the possibility to scale up the process. This technique can produce both MWCNTs and SWCNTs depending on the temperature, wherein production of SWCNTs occurs at a higher temperature than MWCNTs.

2.3. Properties of carbon nanotubes

2.3.1. Electrical properties

Depending on their chirality and diameter, CNTs can be either metallic or semiconducting in their electrical behaviour [20, 27, 51, 52]. In terms of the chiral index, a CNT will be metallic if $|n - m| = 3q$ otherwise, it will be semiconducting [53]. Theoretically, metallic nanotubes can carry an electric current density of 4×10^9 A/cm², which is more than 1000 times greater than those of metals such as copper [3]. Because of its nanoscale cross-section, electrons propagate only along the tube axis. As a result, carbon nanotubes are frequently referred to as one dimensional conductor. The maximum electrical conductance of a single-wall carbon nanotube is $2G_0$, where $G_0 = 2e^2/h$ is the conductance of a single ballistic quantum channel [54].

2.3.2. Thermal properties

All nanotubes are expected to be very good thermal conductors along the tube axis, exhibiting a property known as ballistic conduction, but good insulators laterally to the tube axis [55–58]. A SWCNT has been shown to have a thermal conductivity along its axis of about 3500 Wm⁻¹ K⁻¹ at room temperature [59]. This value is almost 10 times higher than that of copper, a metal well known for its good thermal conductivity which is 385 Wm⁻¹ K⁻¹. A SWCNT has a room-temperature thermal conductivity in the radial direction of about 1.52 W/m/K² which matches very well with the thermal conductivity of soil. The temperature stability of CNTs is estimated to be upto 2800°C in vacuum and about 750°C in air [20].

2.3.3. Mechanical properties

CNTs are the strongest and the stiffest materials yet discovered in terms of tensile strength and elastic modulus, respectively [20, 27, 60–62]. This strength is a direct consequence of covalent sp² bonds formed between the individual carbon atoms. It has been shown that CNTs are very strong in the axial direction. Young's modulus of the order of 270–950 GPa and tensile strength of 11–63 GPa were obtained [63].

On the other hand, there was evidence that in the radial direction, they are rather soft. The first transmission electron microscope observation of radial elasticity suggested that even the van der Waals forces can deform two adjacent nanotubes [64]. Later, nanoindentations with atomic force microscope were performed by several groups to quantitatively measure radial elasticity of MWCNTs [65, 66] and tapping/contact mode atomic force microscopy was also performed on SWCNTs [65]. The results show that MWCNTs are radially deformable to a large extent notwithstanding their axial rigidity and strength under tensile load.

2.3.4. Magnetic properties

Although pure CNTs are non-magnetic in nature, but the most synthesized CNTs (both SWCNTs and MWCNTs) are known to possess magnetic properties that can be attributed to the presence of entrapped catalyst nanoparticles in their inner cavity. Such catalytic particles are formed either in situ during the growth of CNTs (e.g. from ferrocene during MWCNTs

synthesis by CVD) or from previously added metallic catalyst particles (e.g. from Fe-, Co- or Ni-filled electrodes during MWCNTs/SWCNTs synthesis via arc discharge). In general, SWCNTs tend to have very high amount of catalytic residues and possess stronger magnetic character than MWCNTs. As the magnetism is due to the metallic impurities, CNTs tend to lose magnetic character upon treatment under harsh conditions, for example acidic treatment such as functionalization [27, 67] or high-temperature annealing [68].

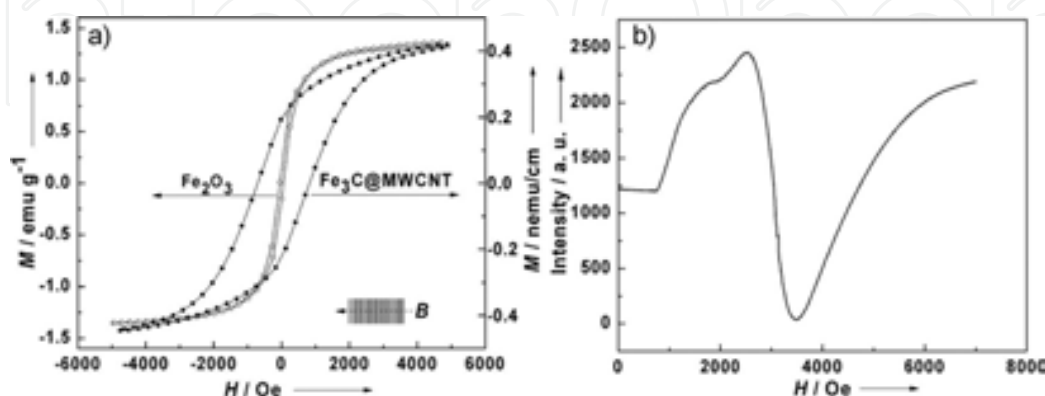


Figure 6. (a) M versus H curves for Fe_2O_3 nanoparticles and $\text{Fe}_3\text{C}@$ MWCNT (B indicates magnetic field, lines the nanotubes, and arrow the direction of the magnetic field). (b) EPR spectrum of $\text{Fe}_3\text{C}@$ MWCNT. Reproduced from [69] with permission from Wiley.

Nevertheless, the CNTs display ferromagnetic behaviour (**Figure 6a**) marked by the presence of hysteresis loop (i.e. nonzero corecivity and retentivity values) [69]. The ferromagnetic nature of CNTs is also supported by the electron paramagnetic resonance (EPR) spectra (**Figure 6b**), showing the presence of a high density of delocalized π electrons corresponding to g values of 2.1365 and 2.2132 for the first and second peaks, respectively. The obtained g values are very near to the characteristic g values of ferromagnetic materials. It is suggested that presence of iron catalyst inside CNTs may be helpful in their magnetic manipulation, for example for magnetic alignment of CNTs in composites [20, 70] or for targeted drug delivery [69]. Further, the magnetic properties also contribute towards electromagnetic energy absorption and play a role in improving its contribution towards total microwave shielding effectiveness [21, 71].

2.3.5. Surface properties/wettability characteristics

The pure CNTs are made up of graphitic cylindrical walls made up of carbon atoms. Therefore, being of non-polar in nature, the surfaces of CNTs (especially MWCNTs) are highly hydrophobic in nature with good affinity towards non-polar materials such as hydrocarbons, paraffins, oils or organic solvents. As CNTs also display relatively high-specific surface area, when 3D shape architected, due to the inherent hydrophobicity they can be useful for water purification applications, for example for separation of non-polar pollutants such as oils, solvents or even organic dyes.

Owing to their chemical inertness, CNTs are difficult to disperse in water and in organic media, and they pose high resistance to wetting. Historically, unlike fullerenes, their chemistry was

considered very poor for a long time. Difficulties also arise in making composites of such inert nanotubes with other materials which is important for many device applications. A suitable functionalization of the nanotubes (i.e. the attachment of 'chemical functionalities') represents a strategy for overcoming these barriers and has thus become an attractive field for synthetic chemists and materials scientists.

3. Functionalization of carbon nanotubes

Functionalization enhances the solubility and processibility, and allows combining the unique properties of nanotubes with those of other materials [20, 26, 27, 72]. It also improves the interaction of the nanotube with other entities, such as a solvent, polymer and other organic molecules and also with other nanotubes. A functionalized nanotube displays different mechanical and electrical properties as compared to pristine nanotube and thus may be utilized for several applications.

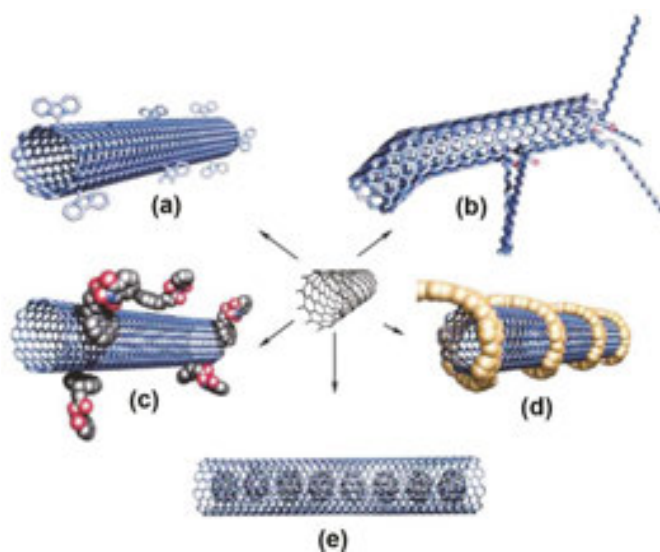


Figure 7. Different possibilities of the functionalization of SWCNTs (a) Sidewall functionalization. (b) Defect-group functionalization. (c) Non-covalent exohedral functionalization with molecules through π -stacking. (d) Non-covalent exohedral functionalization with polymers. (e) Endohedral functionalization, in this case C60@SWCNT. Reproduced from [73] with permission from Springer-Verlag Berlin.

The process of functionalization can conveniently be divided into three major types depending upon the chemistry involved (**Figure 7**) [73].

3.1. Covalent functionalization

Covalent functionalization utilizes the covalent linkage of functional entities onto the nanotube's carbon scaffold. Depending upon the site of interaction, it can be of two types—covalent sidewall functionalization and defect functionalization. Direct covalent sidewall functionalization involves a change of hybridization from sp^2 to sp^3 and the loss of conjugation. Defect

functionalization is based on the transformations of defect sites already present. Defect sites can be the open ends and holes in the sidewalls, terminated, for example by functional groups and Stone/Wales defects (5–7 defects) in hexagonal graphene framework. In addition to these, oxidative purification generated oxygenated sites are also considered as defects. SWCNTs demonstrate low dispersability, and they occur in the form of bundles. This situation warrants the use of a highly reactive reagent for the covalent bond formation at the sidewalls. It is not possible to tell beforehand that whether these addition reactions are more likely to take place at defect sites or intact hexagonal regions of sidewall. Several covalent routes have been taken for covalent functionalization such as oxidative purification [74, 75], amidation [76], esterification [77], thiolation [78], halogenation [79–81], hydrogenation [82], cycloadditions [81, 83–87], electrochemical functionalization [88, 89].

3.2. Non-covalent functionalization

Covalent functionalization suffers from the drawback of damaging the structure of CNTs. Therefore, with a view to retain the structural integrity and π network of CNTs, non-covalent functionalization is particularly attractive. The adsorption forces, such as van der Waals' and π -stacking interactions, are responsible for the non-covalent interaction between surface active reagents and CNTs. Broadly, surfactants and polymers are utilized for this non-destructive functionalization of CNTs. Surface active molecules such as sodium dodecylsulfate (SDS) or benzylalkonium chloride have been successfully used for the formation of non-covalent aggregates [90–92]. On the other side, polymer wrapping around CNTs can be accomplished through the use of polymers such as poly (*m*-phenylene-*co*-2, 5-dioctoxy-*p*-phenylenevinylene) (PmPV, 2) in organic solvents such as chloroform. The stable solution of the SWNT/PmPV complex exhibits conductivity eight-times higher than that of PmPV, without any compromise on its optical properties. The polar side-chain polymers such as polyvinylpyrrolidone (PVP) or polystyrenesulfonate (PSS) give stable solutions of the SWNT/polymer complexes in water [93].

The covalent and non-covalent functionalizations are essentially exohedral derivatizations.

3.3. Endohedral functionalization

The hollow inner cavity of SWCNTs serves as a capillary for the storage of nanoparticles and fullerenes, etc. The rich endohedral chemistry of SWCNTs is amply illustrated by the incorporation of fullerenes and metallofullerenes in their cavity [94, 95].

4. CNTs-based polymer composites

The spectacular properties of CNTs such as their high strength and stiffness make them ideal candidates for structural applications. At present, polymer nanocomposite is one of the biggest application areas for CNTs. The extraordinary properties of CNTs coupled with easily tailorable characteristics of polymers give rise to truly versatile CNT-polymer nanocomposites [20, 21, 26, 27, 96–106]. The emergence of CNTs as filler materials has contributed in the

realization of CNT-polymer nanocomposites as next generation advanced structural material. Keeping in view, the ubiquitous need for the creation of materials with tailored properties for various applications, it is hardly an exaggeration to call the present age as the 'age of composites'.

By definition, a composite is a multiphase material formed from a combination of materials which differ in composition or form, retain their own chemical and physical properties, and maintain an interface between components which act in concert to provide improved specific or synergistic characteristics not obtainable by any of the original components acting alone [20, 107, 108]. Any composite is composed of two categories of materials: the reinforcement or filler and the matrix. The reinforcements contribute useful properties (mechanical, electrical, thermal, optical, etc.) to enhance the matrix properties. In the past decades, we have reached the technological design limits of optimizing composites with traditional micro-meter scale fillers/reinforcements. The limitations of traditional micrometer-scale polymer composites have prompted a considerable research effort to focus on polymer nanocomposites. This new hopes-laden advancement over the traditional polymer composites is characterized by the presence of at least one phase which is less than 100 nm in at least one dimension. Historically, nanocomposites are not entirely new as some nanocomposites such as carbon black and fumed silica-filled polymers [109, 110] have been used a long time ago. However, the discovery of CNTs added an additional impetus in the polymer nanocomposite research promising hitherto unknown potential for various applications. **Table 1** shows a comparison between various fibre reinforcements and carbon nanotubes in terms of various parameters.

Fibre	Diameter (μm)	Density (g/cm^3)	Tensile strength (GPa)	Modulus (GPa)
Carbon	7	1.66	2.4–3.1	120–170
S-glass	7	2.50	3.4–4.6	90
Aramid	12	1.44	2.8	70–170
Boron	100–140	2.50	3.5	400
Quartz	9	2.2	3.4	70
SiC fibres	10–20	2.3	2.8	190
SiC whiskers	0.002	2.3	6.9	–
Carbon NTs	0.001–0.1	~1.33	Up to ~50	Up to ~1000

Credit: Fisher/ Northwestern University.

Table 1. Comparison and contrast of advanced fibre reinforcements vs. carbon nanotubes in terms of diameter, density, tensile strength and modulus.

4.1. Nanocomposite fabrication methods

A variety of synthesis techniques are in practice for incorporation of CNTs into various polymeric host matrices [14, 20, 21, 26, 27, 97, 108, 111–114]. The main motive is to deagglomerate the CNTs and realize their uniform dispersion inside polymer matrix. Currently, there

is no single technique which is universally applicable to all the situations. Depending upon the thermal or chemical properties of matrix polymer, ease of its synthesis from suitable monomer, desired performance indices of composites and cost constraints, with some trade-off in properties, one can choose the suitable processing method for a particular case. This section briefly describes the important processing techniques for synthesis of CNT-based polymer nanocomposites.

4.1.1. Solution processing

The solution processing is the most common technique to form CNT-based polymer nanocomposites which exploits intensive agitation (e.g. refluxing, mechanical/magnetic stirring, vigorous shaking, high shear homogenization, bath/probe sonication) aided rigorous and thorough mixing of CNTs with polymer in a solvent, so as to facilitate nanotube de-bundling and their dispersion inside host polymer matrix [20, 21, 27, 108, 114]. It is important to note that this technique is limited to the polymers which are soluble in solvent(s).



Figure 8. Schematic representation of solution processing method.

Typical process involves dispersion of nanotubes in a suitable solvent and mixing with the polymer solution (**Figure 8**), followed by film casting and solvent evaporation leaving behind nanocomposite film/sheet. The choice of solvent is mainly governed by solubility of matrix polymer. Further, the solvent for CNTs and polymer dispersion may be same or different, but should be of good miscibility to realize intimate mixing between phases. In many cases, CNTs are not separately dispersed rather they are directly added to polymer solution followed by intensive mixing before film casting. The major shortcoming associated with the usage of high-power ultrasonication or shear mixing for a long time is that it can lead to the shortening of tube lengths, thereby deteriorating the composite properties. Plenty of literature [14, 21, 97, 106, 114–119] is available on the formation of CNT-based nanocomposites by this method using both organic as well as aqueous media and variety of polymer matrices [14, 21, 120–123]. To enable better dispersion and to solve the problem of tube shortening upon high-power agitation, some efforts have been made to use surfactants for tube dispersion or to use physically/chemically functionalized CNTs [120, 124, 125]. However, the use of surfactant carries the unavoidable limitation of retaining surfactant in the nanocomposites which hinders the thermal/electrical transport properties of nanocomposites [120]. In contrast, the functionalized CNTs often provide positive results in terms of CNTs deagglomeration, dispersion and their improved interfacial adhesion with matrix polymer, which gets reflected in terms of

superior electrical, thermal, mechanical and dielectric properties of resultant nanocomposites [14, 27, 106, 114]. The boiling point of dispersion medium or solvent (s) is found to have a profound impact on the properties of formed nanocomposites [14, 27, 114, 121]. In general, low-boiling point (i.e. fast evaporating or drying) solvents are preferred, due to their ease of removal from the solution-casted nanocomposites mass. In contrast, high-boiling point solvents are difficult to be removed and tend to get trapped in the solidifying/curing mass. Such a trapped solvent may interfere with the curing reaction (in thermosets) or can act as softener (in thermoplastics), thereby adversely affecting electrical, thermal or mechanical properties. In addition, efforts to remove the solvent and to prevent evaporation generated voids formation add towards complexity and cost in terms of requirement of systems for controlled heating, vacuum/pressure [14]. Another, limitation encountered quite often with solution processing is that the slow evaporation of solvent provides sufficient time for CNTs re-agglomeration and differential settling, resulting in inhomogenous CNTs dispersion in matrix (e.g. CNTs content lowest at the casted film/sheet's surface, shows a uniform/random gradient across thickness and maximum at both surfaces due to the extensive tube settling) and observation of non-uniform and inferior properties. The solvent evaporation rate-related limitations can be resolved by gently pouring CNT/polymer nanocomposite dispersion on a rotating substrate (spin coating) [122] or over a heated substrate (drop-casting) [126]. However, use of spin coating is limited only to thin films (few nanometres thick) which cannot be peeled off from the substrate, whereas drop casting has issues in terms of uniform drying across thickness and high possibility of void formation. Another versatile method exploits coagulation [114, 123, 127] of CNT/polymer dispersion by pouring into an excess of non-solvent, thereby achieving rapid precipitation of polymer chains which immediately entrap CNTs (without providing sufficient time for CNTs diffusion and settling). Nevertheless, solution processing is still widely used and is one of the important steps in the processing of thermo-setting matrices-based nanocomposites.

4.1.2. Melt processing

The melt processing is considered as viable option for making thermoplastic matrices-based CNT/polymer composites due to its low cost and amenability towards large scale synthesis for industrial applications. Here, elevated temperatures are exploited to melt the receptor thermoplastic matrix polymers, which form a viscous liquid and made to flow [21, 26, 108, 114, 128]. The molten polymer flow induces high shear forces which assist in partial de-agglomeration of CNTs bundles and their dispersion inside matrix. The melt mixing can be carried out in batch or continuous operation using high shear mixer (e.g. Sigma mixer) and extruder, respectively. Sigma mixer is often used to prepare highly concentrated nanocomposites called masterbatches, which maybe used to synthesize desired CNTs-loading composites by their mixing with proportionate amount of neat matrix polymer using extruder. An extruder may consist of single or twin screws with twin screw version being more effective in terms of mixing uniformity and properties. A typical twin screw extruder (**Figure 9**) consists of two co- or counter-rotating screws inside barrel housing. The polymer granules are caught by the rotating screws and pushed forward; they become melted inside heated melting (feed) zone due to the externally provided heat and shearing of the material between screw and barrel. The CNTs

are loaded into the extruder via separate hopper, such that melt-phase mixing takes place due to the combination of shearing and kneading action, and by the time molten-mixture reaches the homogenization zone, it has already achieved significant degree of mixing. Finally, mixture passes to die before coming out as semisolid strands, which may be cooled (via air drying or by passing through water bath) and chopped into granules for further use, for example for compression moulding. The extruded output may also be diverted to injection moulding machine to form desired shape samples.

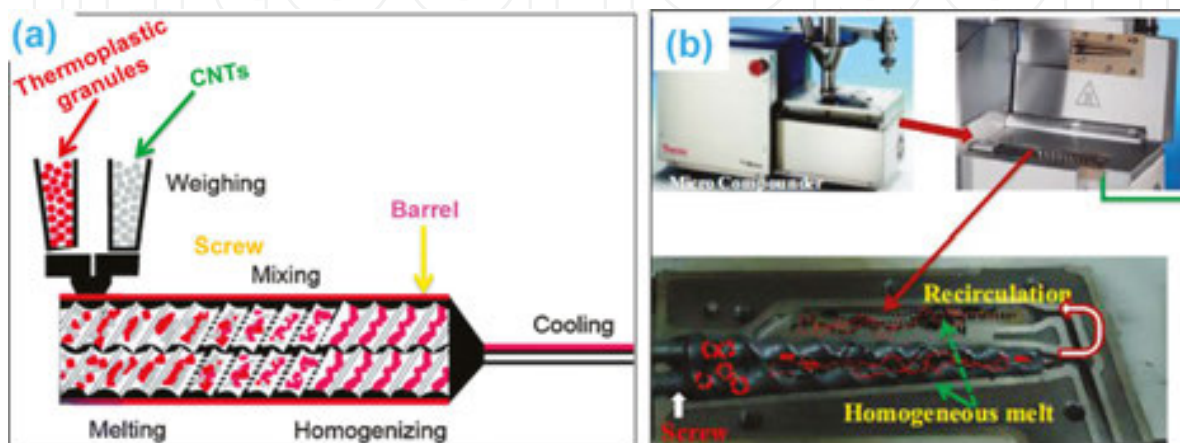


Figure 9. Schematic representation of twin screw extruder for melt phase mixing of CNTs with thermoplastic matrices. Reprinted from [108] with permission from Wiley. (b) Twin screw extruder with melt recirculation provision. Reprinted from [129] with permission from Elsevier.

In the past, melt mixing/blending is successfully exploited for dispersion of CNTs inside various thermoplastic matrices, for example polystyrene [130], polypropylene [130, 131] and acrylonitrile-butadiene-styrene (ABS) [22, 130], polyamide-6 [22], polyethylene [132]. Although melt-mixing technique is simple but the issues of high shear force and elevated temperature need to be properly addressed in order to avoid the deterioration of nanocomposites. While high shear force facilitates CNT dispersion, it can also lead to the undesirable CNT fragmentation or even polymer chain scission. Therefore, the shear force needs to be optimized to achieve desired dispersion without compromising the structural integrity of CNTs. Similar situation prevails with high temperature which promotes CNTs dispersion but can degrade the intrinsic properties of polymer making the need of optimizing the temperature indispensable. Further, it is found that melt-mixing technique is not much effective in breaking of agglomeration of CNTs compared to solution processing [131, 133]. Besides, the melt-mixing fails to realize dispersion of high loading (>5 wt%, which are required for thermal/electrical/electromagnetic applications) inside polymeric matrices, due to the viscosity buildup and screw rpm/reside time limitations [129]. Recently, the above issues are resolved by using a twin screw extruder equipped with melt recirculation provision (**Figure 9b**) [128, 129], such that upto 10 wt% CNTs can be loaded inside polypropylene copolymer (PPCP) matrix without any deleterious effect on mechanical properties.

4.1.3. In situ polymerization

In situ polymerization [14, 21, 108] remains the only viable option for the preparation of composites based on insoluble or thermally unstable matrix polymers, which cannot be processed by solution or melt processing routes. However, many a times, it is used in other cases too (where above limitations are not applicable), due to the distinguished advantages of in situ polymerization in terms of ability to allow formation of high CNTs-loading nanocomposites, facilitating good CNTs dispersion within polymer matrix and ensuring excellent intimacy between CNTs and matrix polymers.



Figure 10. Schematic representation of in situ polymerization process.

This strategy involves dispersion of CNTs in monomer (**Figure 10**) followed by in situ polymerization leading to the formation of CNT/polymer nanocomposites. Exploitation of functionalized CNTs or use of monomer-grafted CNTs are known to improve the initial dispersion of the nanotubes in the monomer and consequently in the formed nanocomposites. This results in a stronger and more active interface between nanotube and polymer which is pivotal to the nanocomposite performance for structural, electronic, electromagnetic or electrochemical applications. This method has been used to synthesize CNTs-filled composites with various polymers, for example thermoplastics, thermosets or conjugated polymers-based matrices [14, 21, 26, 27, 111, 112]. In addition to composite formation, in situ polymerization is also used for physical functionalization of CNTs (via surface polymer wrapping), for their onward use as hybrid filler for nanocomposites.

4.1.4. Miscellaneous routes

In addition to aforementioned methods, some other less popular methods are also available for CNT-polymer nanocomposites preparation, for example wet spinning [134], batch mixing inside banbury mixer [129], twin screw pulverization [135], electrophoretic deposition [136] and latex processing [137], twin screw extrusion complemented by melt-recirculation provision [129]. The issue of the synthesis of CNT-based polymer nanocomposites is still an open arena as no single technique is entirely satisfactory on all grounds. Therefore, some efforts have also been made to use combination of techniques, for example solution processing with melt mixing [133]; in situ polymerization with solvent processing [23]; or in situ polymerization with melt processing [114].

5. Properties of CNT/polymer nanocomposites

With the advent of CNTs on technological landscape, there are now myriad possibilities for tailoring the properties of CNT/polymer nanocomposites. The electrical, thermal, dielectric, rheological and mechanical properties of CNTs filled nanocomposites are significantly enhanced compared to neat polymers. However, the issue of property enhancement is a challenging one as the improvement in one property might come at the cost of other. A number of factors such as the nature of matrix polymer, aspect ratio or actual length/diameter of CNTs, its pretreatment (e.g. covalent functionalization, surface coating of polymer or surfactant), loading level, exploited processing technique and the presence of tertiary phase (e.g. compatibilizer) are known to exert decisive influence on the properties of formed nanocomposites. The next section briefly describes the important properties of CNT/polymer nanocomposites.

5.1. Electrical properties

The very high intrinsic conductivity and low aspect ratio (length/diameter ratio) of CNTs compared to other carbon-based fillers (e.g. carbon black, graphite, carbon fibre), inspired researchers to synthesize CNTs filled electrically conducting nanocomposites. The incorporation of CNTs leads to onset of electrical conductivity within otherwise insulating matrix. This can be attributed to formation of 3D electrically conductive networks within host thermoset matrix so that electrons can easily hop/tunnel between dispersed filler particles [23]. The minimum filler loading where first continuous network of filler particles were formed within matrix polymer is known as percolation threshold. At this point, electrical conductivity of composites displays a sharp rise, that is several orders of magnitude (**Figure 11a**).

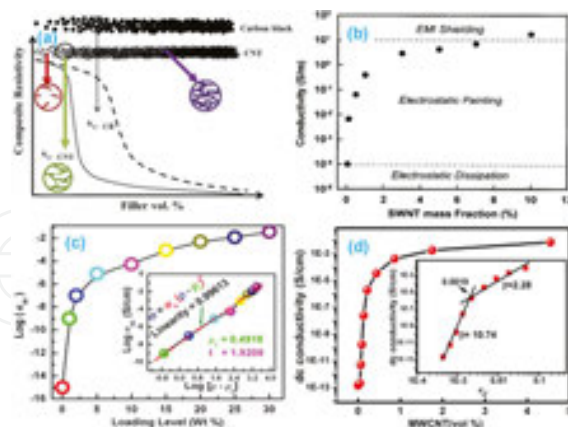


Figure 11. (a) Schematic representation of difference between percolation behaviour of CNTs compared to carbon black. (b) Electrical conductivity of SWNT/polycarbonate nanocomposites as a function of nanotube loading, showing a typical percolation behaviour. Dashed lines represent the lower limits of electrical conductivity required for the specified applications. Reproduced from [138] with permission from AIP. (c) Variation of conductivity (σ_{dc}) of PANI-MWCNT nanofiller-loaded polystyrene solution blends. Inset shows the percolation and scaling details. Reproduced from [23] with permission from Elsevier (d) Plot of electrical conductivity (σ) versus MWCNT (vol%) for PPCP/MWCNTs composites. Inset shows the log-log plot of σ as a function of (v_c). Reproduced from [129] with permission from Elsevier.

Depending upon the level of achieved electrical conductivity, these conductive nanocomposites may have a multitude of applications (**Figure 11b**) including electromagnetic interference (EMI) shielding, transparent conductive coating, electrostatic painting and electrostatic dissipation [138, 139]. Especially, electrically conductive CNT-polymer composites are used in anti-static packaging applications, as well as in specialized components in the electronics, automotive and aerospace sectors.

The critical conducting filler loading (i.e. percolation threshold) for a given matrix-filler combination can be calculated by plotting the electrical conductivity as a function of the reduced volume fraction of filler (**Figure 11c**) and performing data fitting with a power law function [23]:

$$\sigma = \sigma_o (v - v_c)^t \quad (1)$$

where σ is the electrical conductivity of the composite, σ_o is characteristic conductivity, v is the volume fraction of filler, v_c is volume fraction at the percolation threshold, and t is the critical exponent. The $\log(\sigma)$ versus $\log(v - v_c)$ plot (inset, **Figure 11c**) gives a straight line according to Eq. 10. In practical situations, where the densities of polymer matrix and filled inclusion are same (e.g. for organic fillers like ICPs, CNTs or graphene), the mass fraction, p , and volume fraction (v) of the filler can be assumed same. The percolation threshold can also be determined by plotting the $\log(\sigma)$ versus $\log(v)$ plot and finding the point of intersection of lines (**Figure 11d**) corresponding to different (β) values.

The CNT/polymer composites show very low percolation threshold for electrical conductivity [14, 27, 114]. For SWCNT/polymer composites, the percolation thresholds ranging from 0.005 vol% to several vol% have been reported [140]. On the other hand, in case of MWCNT/polymer composites percolation threshold up to 0.002 vol% has been reported [141]. It is found that compared to common conductive fillers, for example metallic or graphitic particles in any shape (spherical, platelet-like or fibrous) and size, CNTs display much lower percolation threshold (**Figure 11**). This can be ascribed to combination of their high inherent conductivity and very high aspect ratio.

It is found that the percolation threshold in CNT/polymer nanocomposites depends on several parameters viz. dispersion [14, 20, 27, 114, 124], alignment [14, 21, 106, 123, 129, 133, 142], aspect ratio [140, 143]. Higher aspect ratio is obtained for well-dispersed nanotubes relative to nanotube bundles making percolation threshold decrease with better dispersion. Bryning et al. [140] reported a smaller percolation threshold with the higher aspect ratio nanotubes for SWCNT/epoxy composites. The percolation threshold is also significantly affected by alignment of the nanotubes in the polymer matrix. In the alignment condition, there are fewer contacts between the tubes which results in a reduced electrical conductivity and a higher percolation threshold as compared to random orientation of nanotubes. It is a common notion that chemical functionalization reduces the electrical conductivity of nanotubes through disruption of the extended π -conjugation of nanotubes. However, it is also reported that functionalization can improve the electrical properties of the composites [144–147]. Valentini

et al. [146] concluded that the amine-functionalized SWCNT in epoxy matrix allows migration of intrinsic charges raising the conductivity of the composite. Similar result is also obtained by Tamburri et al. [147] for the functionalization of SWCNT with hydroxyl and carboxylic groups in 1,8-diaminophthalene. Therefore, it is established that negative effects of functionalization for SWCNTs conductivity are often counterbalanced by the improved dispersion caused by functionalization, with overall effect leading to positive outcome.

5.2. Thermal properties

Due to the excellent thermal conductivity of CNTs, some efforts have been made to incorporate them into various polymer matrices to improve thermal conductivity of formed composites [148–153]. It is found that, besides CNTs content, the thermal conductivity of CNT/polymer nanocomposites also depends on state of their dispersion and alignment as well as aspect ratio and the presence of metal impurities. Biercuk et al. [150] synthesized an epoxy composite with 1 wt% raw laser-oven SWCNTs that showed a 125% increase in thermal conductivity at room temperature. Choi et al. [154] reported a 300% increase in thermal conductivity at room temperature with 3 wt% SWCNTs in epoxy. They also obtained an additional 10% increment in case of magnetic alignment. Du et al. [155] reported an infiltration method with an epoxy and a nanotube-rich phase showing a 220% increase in thermal conductivity at 2.3 wt% SWCNTs loading. Among various CNTs variants (SWCNTs, MWCNTs, DWCNTs) in epoxy composites, the MWCNTs are found to most significantly improve the thermal conductivity of polymer composites. This is due to their relatively low interfacial area (therefore, less phonon scattering at the interface) and the existence of shielded internal layers which promote the conduction of phonons and minimizes the matrix coupling losses [149]. Besides, thermal conductivity improvement, CNTs are also known to improve the thermal stability of the polymer composites. This may be attributed to better heat dissipation characteristics. Nevertheless, these good thermal conductivity nanocomposites are considered very promising candidates for a number of applications such as thermal interface materials, heat sinks, printed circuit boards, connectors and other high-performance thermal management systems.

5.3. Mechanical properties

The outstanding intrinsic mechanical properties of CNTs (including ultra-high-specific strength and modulus) make them especially lucrative as fillers in CNT-polymer nanocomposite materials. Due to these properties, only they were talked about as filler material for composite cables for NASA's fascinating project of space elevator [156]. Therefore, several efforts have been made in the past, to translate the fraction of exceptional mechanical properties of CNTs into formed nanocomposites.

In general, the tensile modulus and strength of CNT-polymer nanocomposites increase with nanotube loading (**Figure 12a–c**), dispersion, and alignment in the polymer matrix [14, 20, 21, 27, 114, 128, 129] However, unlike modulus (**Figure 12c**), the tensile strength (**Figure 12b**) does not follow a monotonic increase [14, 20] with CNTs loading, due to CNTs re-aggrega-

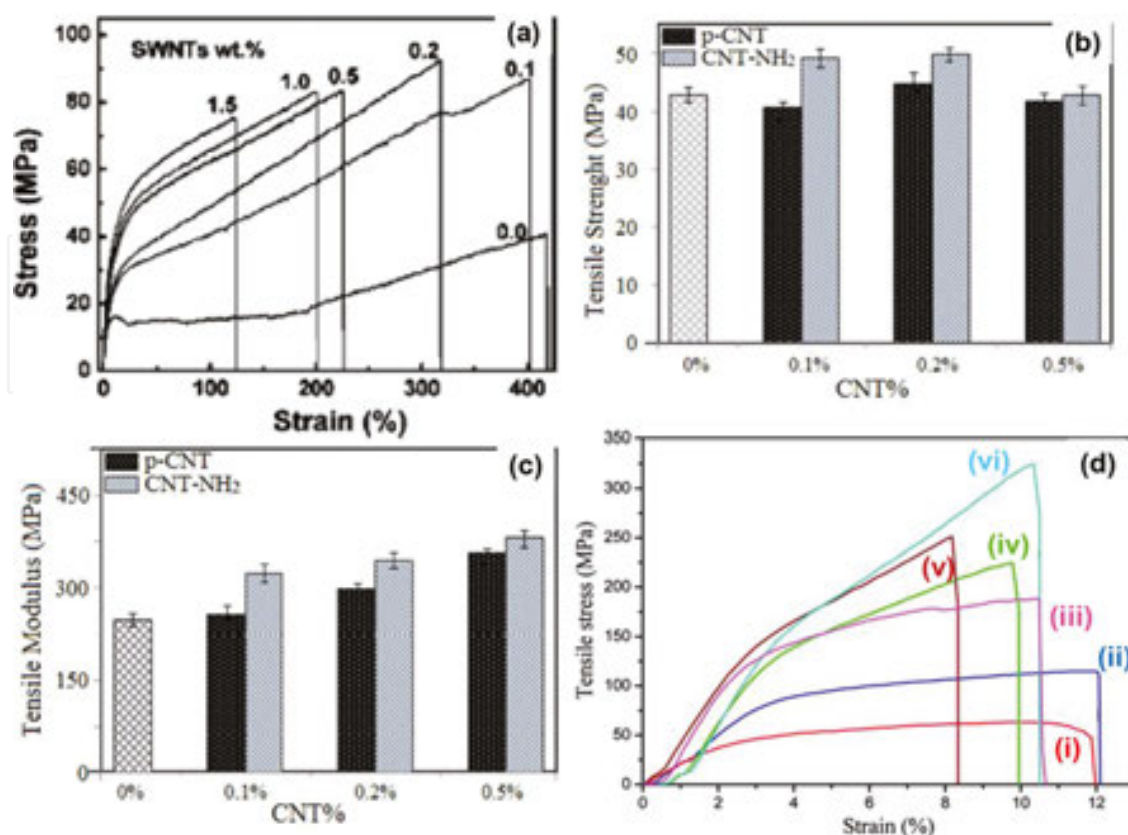


Figure 12. (a) Stress–strain profiles of SWNT-nylon-6 composite fibres at different SWCNT loadings. Reproduced from [157] with permission from ACS. (b) Tensile strength and (c) tensile modulus of epoxy nanocomposites containing various % loadings of pure CNTs (p-CNT) and amino functionalized (CNT-NH₂). Reproduced from [158] with permission from ACS. (d) Typical stress–strain curves for (i) electrospun pure PAN terpolymer nanofibre sheets; (ii) electrospun PAN terpolymer nanofibre sheets with 2 wt% loading of grafted MWCNTs; (iii) hot-stretched pure PAN terpolymer nanofibre sheets; (iv–vi) hot-stretched PAN terpolymer nanofibre sheets with 1, 2 and 3 wt% loadings of grafted MWCNTs, respectively. Reproduced from [159] with permission from ACS.

tion, viscosity buildup issues, incomplete CNTs wetting by polymer and their poor dispersion. Therefore, optimum CNTs loading and means to overcome above negative factors are keys towards realizing composites with good mechanical properties. It is observed that the theoretical predictions of mechanical properties and experimental findings often differ due to the number of issues including the presence of voids, lack of perfect orientation, poor filler dispersion and insufficient load transfer due to the lack of interfacial adhesion. Moreover, nanotube agglomeration decreases the modulus of the nanotubes compared to that of isolated nanotubes because the nanotubes involve only weak dispersive forces between them. According to the molecular simulation studies and elasticity calculations done by Liao et al. [160], when the atomic bonding between the nanotubes and the matrix is not present, there are basically two sources of nanotube/matrix adhesion (i) electrostatic and van der Waals interactions and (ii) stress/deformation resulting from the difference in the coefficients of thermal expansion between the filler and matrix. The functional groups on the nanotube sidewalls are known to improve the compatibility with the polymer matrix. This facilitates interfacial load transfer via CNT/polymer bonding leading to improved mechanical proper-

ties [14, 20, 158]. The stress–strain profile of these composites give a 153 and 103% increase in Young’s modulus and tensile strength, respectively (Figure 12a). The importance of CNTs alignment has also been highlighted [20, 114, 159], and it is shown that the aligned CNTs-based nanocomposites (Figure 12d) display better strength and modulus in orientation direction compared to those based on random CNTs alignment. In spite of so many pros and cons, these lightweight yet structurally strong CNTs-based nanocomposites are considered as promising material for structural applications, for example bullet proof garments or body armours, aircraft or automobile parts, industrial components.

5.4. Dielectric properties

It has been demonstrated that the incorporation of CNTs within insulating or conducting polymer matrices leads to improvement of dielectric properties [21, 23]. This can be attributed to the localization of charges at the CNTs/polymer interfaces, resulting in Maxwell–Wagner interfacial polarization. As a result, both real and imaginary permittivity of the polymer composites scales with CNTs loading (Figure 13).

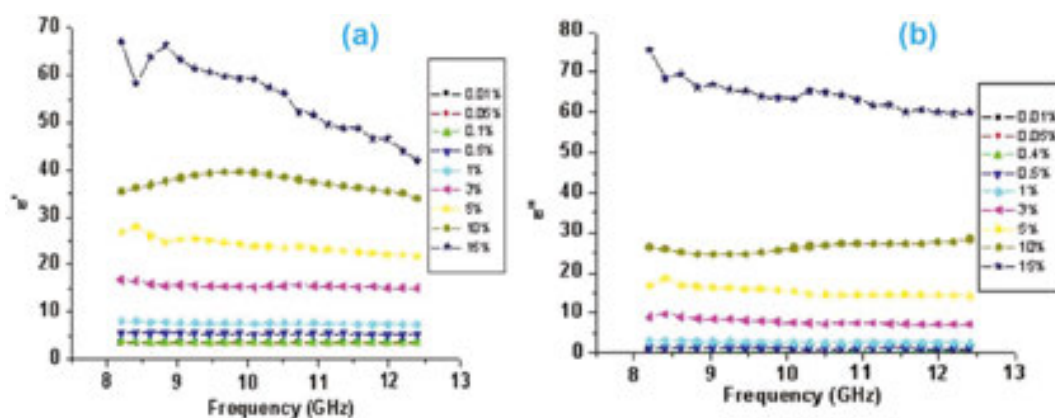


Figure 13. Complex permittivity spectra of the composites using “long-SWCNTs” with loading from 0.01 to 15 wt%. Reproduced from [161] with permission from Elsevier.

The parameter ϵ' (real permittivity) represents the charge storage (or dielectric constant), whereas ϵ'' (imaginary permittivity) is a measure of dielectric dissipation or losses. It is found that dielectric properties are dependent on the CNTs’ aspect ratio, actual length, functionalization/doping status and loading level as well as nature of polymeric matrix and employed processing technique [21, 161]. Such properties are best interpreted in terms of effective medium theory and have direct influence on electromagnetic wave-blocking characteristics of the CNTs/polymer nanocomposites.

5.5. Rheological properties

The rheological properties of CNT/polymer nanocomposites have significance for composite processing as well as a probe of the composite dynamics and microstructure. At high frequencies, the response is almost independent of the filler concentration, indicating that the short-

range polymer dynamics are not influenced by the nanotubes. The glass transition temperatures of the composites remain constant in the absence of strong interfacial bonds and for low nanotube loadings. At low frequencies, with the increase of nanotube concentration, the rheological behaviour gradually shifts from a liquid-like behaviour to a solid-like behaviour. This is in accordance with earlier findings in silicate nanocomposites [162]. Applying a power law function to the data provides a rheological percolation threshold associated with the onset of solid-like response. As observed with respect to electrical percolation, the rheological percolation also depends on aspect ratio, nanotube dispersion and alignment. In a study by Mitchell et al. [163], the effect of dispersion was demonstrated by functionalizing SWCNT such that the rheological percolation threshold decreased from 3 wt% when using pristine SWCNT to 1.5 wt% in functionalized SWCNT/polystyrene composites.

Pötschke et al. [164] also showed the temperature dependence of the rheological percolation threshold. In SWCNT/ PC composite, the percolation threshold decreases from ~5 to ~0.5 wt % MWCNT when the temperature rises from 170 to 280°C. Besides, elucidating structural information, rheological properties also provide useful information about the processability of the nanocomposites.

6. Application of CNT/polymer nanocomposites

As already discussed, incorporation of CNTs inside various polymer matrices enables the formation of advanced nanocomposites with improved or even novel set of electrical, thermal, mechanical, electrochemical or electromagnetic properties. Accordingly, they are known to display a number of dependent applications, which are described in details in the following section.

6.1. Electromagnetic interference (EMI) shielding

The excellent electrical conductivity and high aspect ratio of CNTs compared to other carbon-based fillers (e.g. carbon black, graphite, carbon fibre) and their excellent corrosion resistance, low density along with ultra-high-specific strength compared to metals, inspired the designing of CNTs-based polymer composites. Both SWCNTs- and MWCNTs-based composites have been prepared by their incorporation in various polymer matrices (e.g. insulating thermoplastic or thermosetting polymers, conjugated polymers), and their EMI SE performance was measured [14, 21, 23, 97, 106, 128, 129, 165, 166]. The introduction of CNTs inside host polymeric matrices leads to improvement of electrical conductivity as well as real- and imaginary-permittivity values [14, 21]. These are direct manifestations of increase in number of conducting links and interfacial polarization phenomenon and lead to improvement in SE (Figure 14).

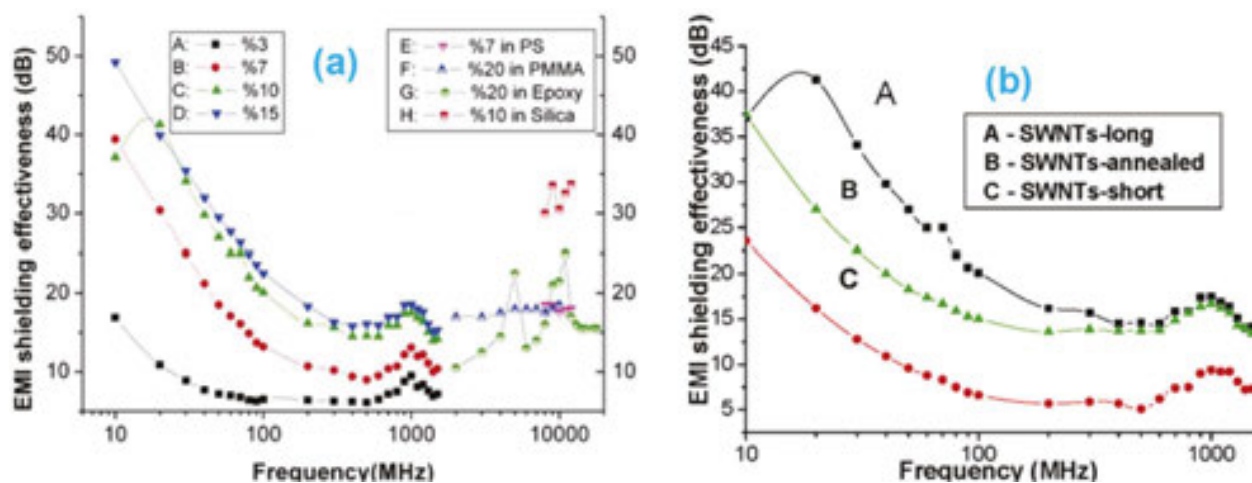


Figure 14. EMI shielding effectiveness (plots labelled A–D) for SWNT-polymer materials (wt% 3–15) studied in this work (10 MHz–1.5 GHz). Plots labelled (E–H) are higher-frequency data on MWNT-based material presented for comparison: (E) MWCNTs in PS; (F) MWCNTs in PMMA; (G) MWCNTs in epoxy resin and the value of the y axis for G is the reflection loss; (H) MWNTs in silica. Impact of wall integrity and aspect ratio on the EMI shielding effectiveness of the composites containing 10 wt% SWCNTs. Reprinted from [166] with permission from ACS.

The SE value also depends upon the nature of polymer matrix (**Figure 14a**), CNT-loading level and state of CNTs de-agglomeration/dispersion. Besides, CNT aspect ratio and wall defects (**Figure 14b**) also play crucial role in deterring shielding performance [14, 166]. In general, composites based on higher aspect ratio CNTs tend to display higher conductivities and better real and imaginary permittivity values compared to low aspect ratio CNTs, which gets reflected in terms of better shielding performance of the former. Further, annealed CNTs (containing very low defects)-based composites display superior shielding performance compared to unannealed CNT-filled composites.

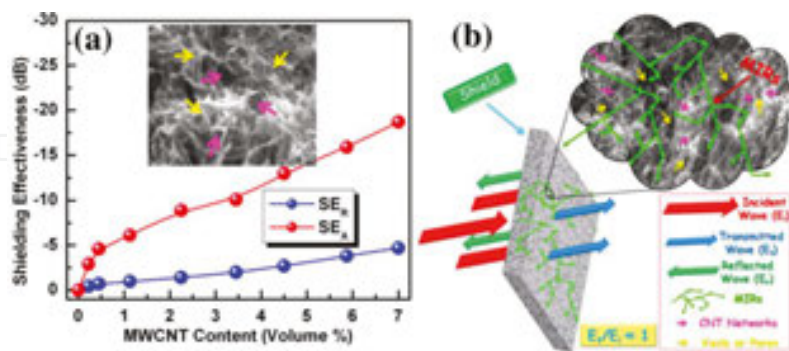


Figure 15. (a) Variation of reflection (SE_R) and absorption (SE_A) losses with MWCNT loading and magnified SEM image (inset) showing dispersed CNTs and voids, (b) Schematic representation of radiation shield interaction and involved multiple internal reflection (MIR) phenomenon. Reprinted from [106] with permission from Springer.

It has also been demonstrated that increased interfacial polarization and improvement of CNT dispersion via surface coating of conducting polymers [23, 106] lead to improvement of shielding response in the composites. It is suggested that CNTs networks inside composites

trigger multiple reflections (**Figure 15b**), which are considered beneficial for improvement of absorption and overall shielding (**Figure 15a**). As the high CNT loading is required (where mechanical properties often degrade due to agglomeration and inhomogeneous filler dispersion issues) for achieving high shielding performance, some efforts have also been made to prepare high CNT loading (>10 wt%) yet mechanically strong composites via melt recirculation aided extrusive mixing [128, 129]. These composites display good shielding effectiveness. Recently, it is shown that at relatively low CNTs loading (<4 wt%), high aspect ratio and long-length CNTs-based composites display better shielding performance, whereas at higher (>4 wt %) CNTs loading, low aspect ratio and low-length CNTs-based composite show superior SE, probably due to the complex interplay between, impedance matching, interfacial polarization and multiple reflection phenomenon [128].

6.2. Supercapacitor electrodes

CNTs, due to their superior electrical properties, good mechanical and thermal stability, readily accessible surface area and unique pore structure are an attractive candidate for supercapacitor electrode applications [167, 168]. The composite formation strategy, involving incorporation of CNTs into various conjugated polymers (e.g. PANI, PPy) matrix, is considered an effective solution for improving the mechanical and electrochemical properties of electrodes [102, 103, 168–171]. For example, the sulfonated multiwall carbon nanotube (MWCNTs) in the composites [102] can greatly improve the cycle stability of PANI (**Figure 16**, left image), only showing 5.4% loss from their initial specific capacitance even after 1000 cycles. This was attributed to the use of MWCNTs with exceptional mechanical properties as a support and the formation of the charge-transfer complex, which could reduce the cycle degradation problems of PANI caused by volume changes or mechanical problems [102, 168]. Similarly, sulfonated-MWCNT/polypyrrole nanocomposite (MWCNTs/C-SO₃H/PPy) [170] exhibited good rate ability, high-specific capacitance (357 F/g), and high-specific capacitance retention rate (specific capacitance loss was only 3% even after the 1000 cycles). Apart from preserving the conducting polymer active material from mechanical changes (such as shrinkage and breaking) during long cycling, CNTs also improved the charge transfer characteristics, thereby facilitating the realization of high charge/discharge rates [103, 171].

It has also been realized that due to their excellent electrical and mechanical properties and open tubular mesoporous network structure, CNTs can act as good support materials for pseudocapacitive materials like conjugated polymers [167, 168]. Zhang and co-workers [167] have reported the use of a carbon nanotube array directly connected to the current collector (Ta foil) as the support to make composite electrodes with hierarchical porous structures. The electrochemical studies have shown that these PANI/CNT composite electrode (**Figure 16**, right image) with nanosize hierarchical porous structure, large surface area, and superior conductivity had high-specific capacitance (1030 F/g), superior rate capability (95% capacity retention at current density of 118 A/g), and high stability (i.e. only 5.5% capacity loss after 5000 cycles) between potential window of -0.2 to +0.7 V (vs. SCE) in 1.0 M H₂SO₄ electrolyte. These results are considered as manifestations of efficient charge transport (in the composite electrode); high-specific capacity (due to the efficient utilization of electrode materials);

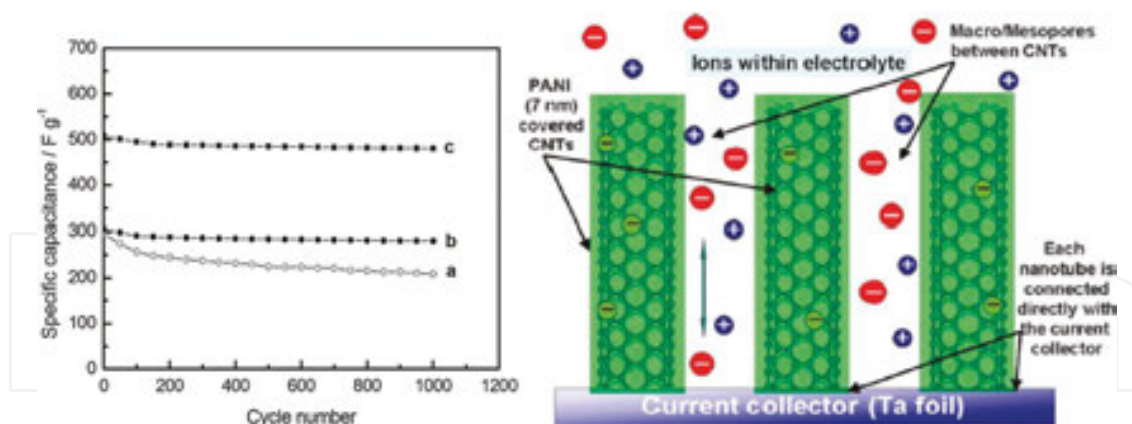


Figure 16 Cycle stability of (a) PANI nanorods, (b) PANI/sMWCNT-2, and (c) PANI/sMWCNT-4 electrodes in the voltage range of -0.2 to 0.75 V at a current density of 1 A/g (left image). Reproduced from [102] with permission from Elsevier. Schematic representation of the microstructure and energy storage characteristics of a polyaniline/carbon nanotube (PANI/CNT) composite electrode (right image). Reproduced from [168] with permission from RSC.

improved ionic conductivity; and countering of mechanical stability problems or volume changes by CNTs. Some efforts have also been made to deposit conjugated polymer over CNTs-based membranes to be directly used in supercapacitor with metal backing. For example, pulsed electrochemically deposited PPy over MWCNT membrane-based electrode [172] displayed remarkable specific capacitance of 427 F/g. Similarly, attempts have also been made to combine composite and paper electrode strategy, for example Oh et al. [173] prepared the highly porous sheets comprised of SWCNT/PPy composite by vacuum filtration of SWCNT/PPy methanol dispersions. The nanotube network provided mechanical strength and improved electrochemical performance of the nanocomposites. The highest specific capacitance of 131 F/g was obtained for nanocomposite with 1:1 SWCNT: PPy ratio.

6.3. Photovoltaics

The excellent electron transport properties of carbon nanotubes (CNTs) and their larger electron affinity compared to available polymer-based light-harvesting donors prompted to use them in bulk heterojunction (BHJ)-type hybrid solar cells. Their acceptor characteristics have been demonstrated by their ability to rapidly quench (at very low CNTs loading) the photoluminescence (PL) of polymer-based donor [100, 101, 174–176] which is a direct evidence of charge transfer from polymer (donor) to CNTs (acceptor). Further, CNTs also act as good transporter for exciton dissociation generated electrons. The initial effort in the direction [39] demonstrated that incorporation of 1% SWCNTs inside poly(3-octylthiophene) (P3OT) donor lead to efficient exciton dissociation and improved open-circuit voltage (V_{OC}). Another study has highlighted the influence of SWCNTs on the crystallinity enhancement and morphology improvement (continuous interpenetrating network formation) in poly(3-hexylthiophene) (P3HT)-based solar cells [176]. It is also outlined that workfunction of P3HT-modified SWCNTs increases due to the shifting of Fermi level towards vacuum level, leading to the improvement of V_{OC} . Another work [174] showed that the solar cells BHJ active layer based on semiconducting SWCNTs (s-SWCNTs)/P3HT blend (**Figure 17a**) form nanofilaments

(Figure 17b) which helps in preventing bundling of s-SWCNT via formation of core shell structures (Figure 17c and inset).

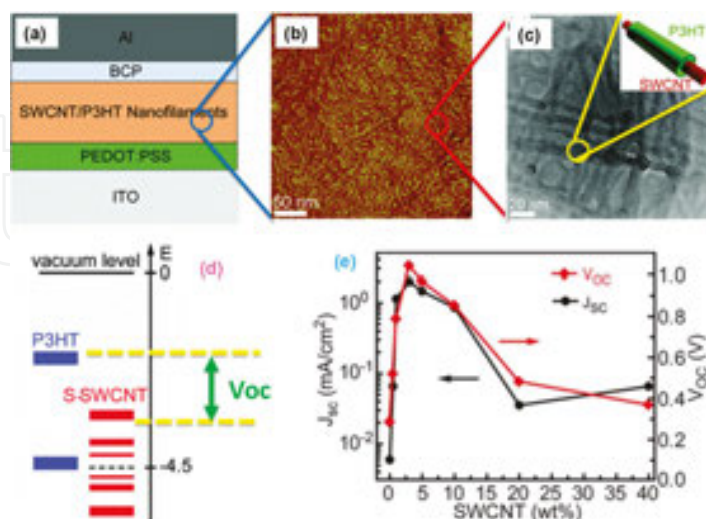


Figure 17. (a) Device structure of SWCNT/P3HT nanofilament BHJ layer-based solar cells. (b) AFM phase image of P3HT/s-SWCNT nanofilaments in a sample with 3 wt% SWCNT showing the worm-like morphology of the active layer. (c) Bright field TEM image of P3HT/s-SWCNTs blend having 3% s-SWCNT and schematic (inset) of P3HT coating over SWCNTs. (d) Band diagram for P3HT/s-SWCNTs interfaces and V_{oc} . (e) Dependence of J_{sc} and V_{oc} on the loading concentration of SWCNTs. Reproduced from [175] and [174] with permission from AIP and ACS respectively.

Such ordered configuration containing synergistic combination of s-SWCNTs and P3HT lead to improvement of charge separation, V_{oc} improvement (Figure 17d) and efficient carrier transport, which collectively contribute towards light-to-electricity conversion efficiency enhancement (Figure 17e). The role of CNT content has also been investigated, and it was pointed that short-circuit current (J_{sc}) and V_{oc} of devices critically rely on the SWCNT loading (Figure 17e). For example, in the present system, both the J_{sc} and V_{oc} display proportionate increases up to 3 wt% (V_{oc} of 1.04 V and J_{sc} of 1.99 mA/cm²) CNT content and decreases afterwards. Duly supported by morphological and electrical studies that was ascribed to the formation of optimal co-continuous interpenetrating-type morphology only around 3 wt% s-SWCNT loading. Above this value, phase segregation takes place, thereby decreasing the exciton breaking and charge transport efficiencies. It has also been shown that P3HT/s-SWCNT BHJs can generate photocurrent from photons absorbed both in the P3HT and in the s-SWCNT and can achieve an IQE of 26% in the near-infrared region. Another work demonstrated that incorporation of MWCNTs into the P3HT/C₆₀ BHJ layer increased the fill factor by 20% with a corresponding improvement of efficiency compared to the polythiophene/C₆₀ bilayer device containing no MWCNTs [175].

6.4. Thermoelectrics

Recently, several attempts have been made to combine the excellent electrical conductivity, tunability of Seebeck coefficient, outstanding mechanical properties and good thermal stability of CNTs with the solution processability, low thermal conductivity, cost advantages and facile

and scalable synthesis of conducting polymers. In particular, nanoscale heterostructuring is considered as good approach to regulate thermopower and electrical/thermal conductivity. In early attempts, conducting polymer/CNTs nanocomposites [105, 177, 178] (e.g. PANI/CNTs and PEDOT/CNTs) were synthesized by in situ polymerization (**Figure 18a**) to introduce heterojunctions and to see the effects of constituents on thermoelectric properties.

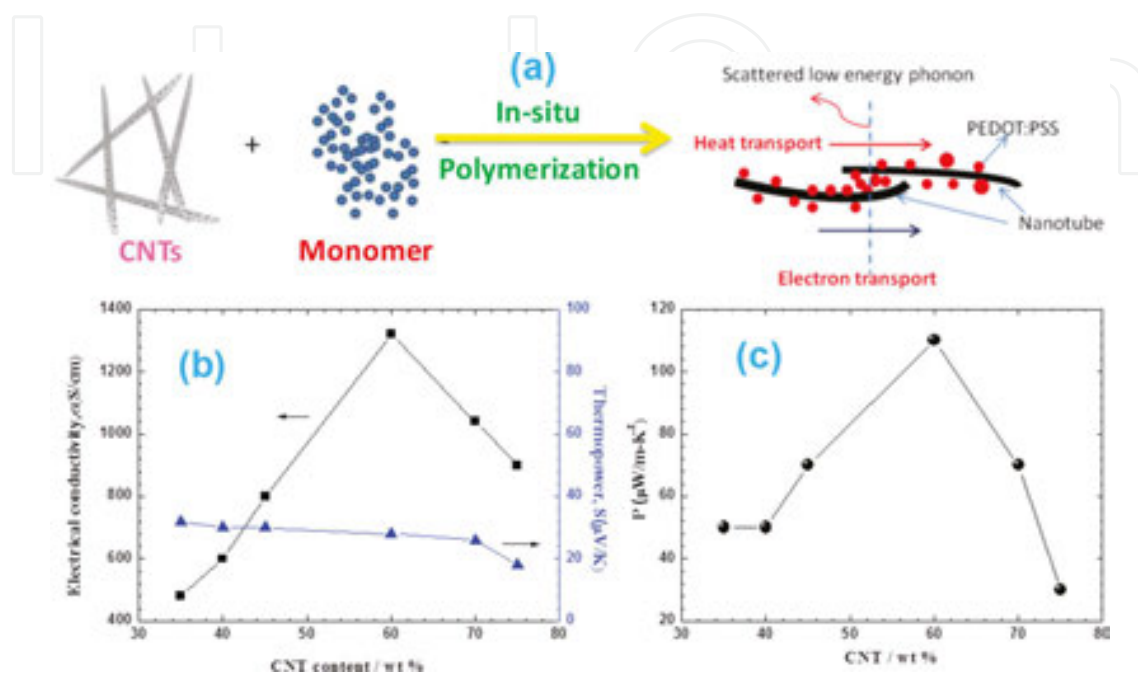


Figure 18. (a) Schematic representation of the formation of CNT/conjugated polymer by in situ polymerization leading to coating of nanotubes by polymer and formation of heat/electricity flow regulating nanojunctions. (b) Electrical conductivities and thermopower (i.e. seebeck coefficient) and (c) Power factor for the CNT/PEDOT-PSS composites. Reproduced from [179] with permission from ACS.

The presence of the heterojunctions is expected to improve the thermoelectric transport properties, that is obstructing the heat flow and favouring the electronic conduction. Indeed, it has been observed that poly(3,4-ethylenedioxy-thiophene)-poly(styrenesulfonate) (PEDOT:PSS)/CNTs composites display improved electrical conductivity without significantly altering or decreasing thermopower (i.e. seebeck coefficient) (**Figure 18b**), ultimately resulting in improved power factor (PF) (**Figure 18c**). This behaviour results from thermally disconnected, but electrically connected junctions in the nanotube network, which makes it feasible to tune the properties in favour of a higher thermoelectric figure of merit [178, 180]. Similarly, when bundle of CNTs were coated and bounded by PANI, the thermally insulating PANI interfacial layer can act as energy filters, which allow the high-energy carriers to pass and scatter the low-energy carriers, thereby increasing the Seebeck coefficient [177]. Furthermore, the growth of PANI over CNTs forms an ordered chain structure [105] which reduced the π - π conjugation defects along the PANI backbone causing increase in carrier mobility (i.e. increased electrical conductivity). As a result, the composite possesses similar thermal conductivity as that of pure PANI (though orders of magnitude lower than pure CNTs) but significantly improved PF compared to pure PANI or CNTs (**Figure 19**)

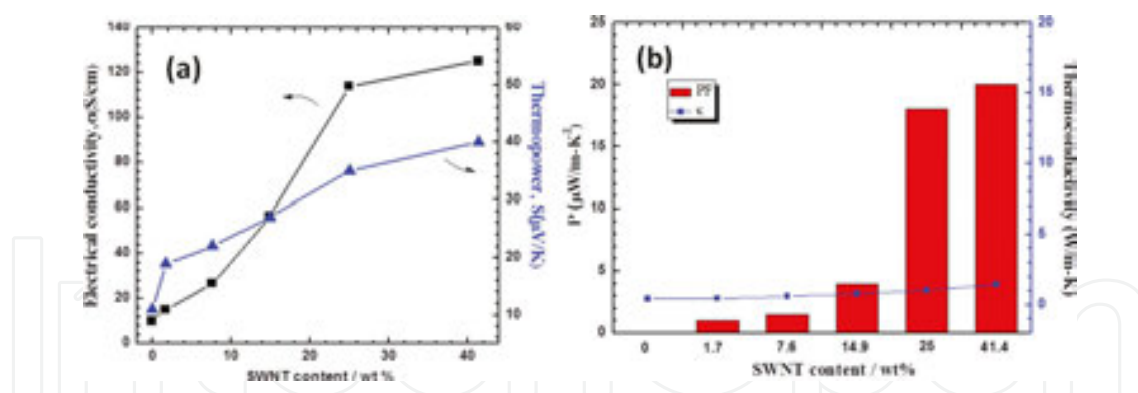


Figure 19. Seebeck coefficient and electrical conductivity (a), power factor and thermal conductivity (b) of SWCNT/PANI composites with different SWCNT content. The dashed line is the calculated electrical conductivity and thermal conductivity based on the particle mixture rule. Reprinted from [105] with permission from ACS.

Besides ordering-induced improvement in carrier mobility, such systems also show anisotropic thermoelectric properties [181] with more than a doubled improvement of power factor in the orientation direction. This provides a novel and effective way of improving the thermoelectric properties of conducting polymers.

In addition to conducting polymers, efforts have also been made to combine CNTs with conventional insulating polymers to improve thermoelectric PF. For example, in polyvinylidene fluoride (PVDF)/SWCNT composite [182] thin films-based systems, due to the decrease in CNTs content (from 100 to 5 wt%), the beneficial effects of increasing Seebeck coefficient and decreasing thermal conductivity were outweighed by negative effect of decreasing electrical conductivity, resulting in an increase in a thermoelectric figure of merit (ZT). Similarly, CNT/poly(vinyl acetate) (PVAc) composites [104] show highest thermoelectric performance at 20 wt% CNTs loading, with an electrical conductivity of 48 S/cm, thermal conductivity of 0.34 W/mK and room temperature ZT value larger than 6×10^{-3} . Besides, in addition to improvement in thermoelectric properties, due to their exceptional mechanical properties CNTs are also expected to improve the mechanical properties of their composite-based thermoelectric materials (both bulk materials and thin films).

6.5. Water purification

In recent past, membrane-based filtration techniques have emerged as potential alternatives for waste water purification applications. Owing to their cost-effective facile synthesis, good thermal stability, high mechanical strength and biocompatibility, polymers such as polysulfone, polyamides, cellulose nitrate, polyethersulfone, membranes are the most promising/preferred. However, due to very small pore size, bacteriological contamination and pore blockings by adsorption of inorganic/organic impurities; low throughput and fouling are the common limitations of these membranes. In this context, CNTs owing to their strong antimicrobial activity, tunable surface chemistry and high mechanical strength have emerged as promising filler candidate for making composite membranes with improved antifouling characteristics and mechanical strength. Shawky et. al. [183] has synthesized a MWCNT/

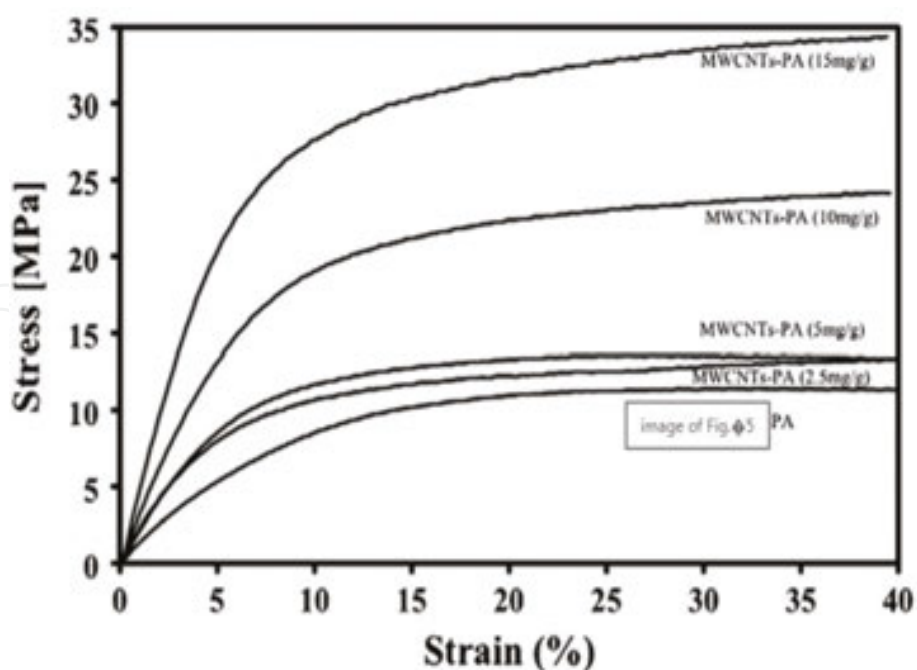


Figure 20. Effect of MWCNTs contents on the stress–strain curves for PA membranes. Reprinted from [183] with permission from Elsevier.

polyamide nanocomposite membrane which exhibited excellent mechanical strength (**Figure 20**) and very good salt rejection ability with high permeability (**Table 2**).

The continuous network formation between structurally compact aromatic polyamide matrix and CNTs is solely responsible for high mechanical strength, good salt rejection ability though at the expense of slightly lower permeability.

MWCNTs loading (mg/g)	Permeability (L/m ² /h bar)	Flux (L/m ² h)	Salt rejection (%)
0	0.76 ± 0.08	32 ± 0.7	24 ± 1.1
2.5	0.75 ± 0.09	32 ± 0.4	28 ± 1.0
5	0.73 ± 0.07	31 ± 1.1	35 ± 0.7
10	0.72 ± 0.10	30 ± 0.9	69 ± 0.9
15	0.71 ± 0.11	28 ± 0.8	76 ± 1.1

Reprinted from [183] with permission from Elsevier.

Table 2. Membrane performance as a function of different MWCNTs loading at constant PA concentration (10%).

However, these membranes suffer from fouling tendency as the incorporation of hydrophobic CNTs in polyamide membranes leads to facile irreversible adsorption of organic/inorganic/biological impurities. It is shown that the fouling problems can be circumvented by altering the surface morphology of the membrane. Since CNTs can be easily transformed from

hydrophobic to hydrophilic by acid treatment; therefore, incorporation of CNTs functionalized with hydrophilic/amphiphilic groups is considered very advantageous for long-term uninterrupted performance of these membranes [184–188]. In this direction, Choi et. al. [187] have fabricated a polysulfone/MWCNT hybrid membrane by phase inversion process. The surface-modified MWCNTs provide hydrophilicity and conductivity to the membrane. The authors reported that the pore size of the membrane increased with increase in CNT loading up to 1.5 wt% but further loading of CNTs increased viscosity of blend solution which led to decrease in pore size. The membrane with 4 wt% of MWCNT has pore size just smaller than pure polysulfone membranes and exhibited higher flux and good salt rejection ability. Nevertheless, the CNTs reinforced polymeric membranes are still a new concept and more efforts in the direction are necessary to further improve their performance and address the negative influence on permeability.

6.6. Gas and chemical vapour sensors

The major drawbacks such as high operating temperature, elevated costs and complex fabrication protocols associated with the conventional metal oxide-based sensors have prompted researchers to look for new avenues to come up with new materials not plagued by these shortcomings. This insatiable quest has unfolded the arena of CNTs-based polymer nanocomposites. The synergistic combination of the remarkable electrical transport and mechanical properties of CNTs and easily tailorable electroactive nature of conducting polymers has the potential to give one of the best-sensing platforms for the efficient gas/chemical vapour detection [99, 189]. Therefore, dedicated efforts have been made to combine CNTs with various conducting polymers such as polyaniline [190–192], poly(3,4-ethylenedioxythiophene)/poly(styrenesulfonate) (PEDOT/PSS)[193], polypyrrole (PPy) [194], hexafluoroisopropanol substituted polythiophene (HFIP-PT), poly(3-hexylthiophene) (P3HT) [195], poly 3-methyl thiophene [98], to fabricate portable, more stable, highly sensitive, cost-effective and energy efficient chemiresistors especially for the detection of extremely minute quantities of environmentally hazardous analytes. In general, incorporation of CNTs tends to improve the mechanical strength, charge transport properties, porosity and specific interactions (due to high-specific surface area available for physico-chemical adsorption) with analytes (gas or chemical vapour), whereas conducting polymer contributes towards electroactivity and improved CNTs dispersion (thus better film formability compared to pristine CNTs). Therefore, the CNTs/conducting polymer nanocomposites often display improved sensitivity, response or selectivity.

The chemical functionalization of CNTs can also help to improve the affinity for one specific analyte species over another during the sensing of analyte mixture. For example, chemically polymerized 3-methylthiophene in the presence of COOH-functionalized MWCNTs, mixed with polyethylene oxide (used as a binder) deposited between two palladium electrodes was sensitive to chloromethanes (CH_3Cl , CH_2Cl_2 , CHCl_3 , CCl_4 , CH_4) with fast response times [98]. However, it was not sensitive to acetone, acetaldehyde, benzaldehyde, tetrahydrofuran, methanol, and ethanol vapours providing high selectivity. The functionalized carbon nanotubes (CNT) with acidic groups (e.g. $-\text{COOH}$) have capability to doped PANI and can improve

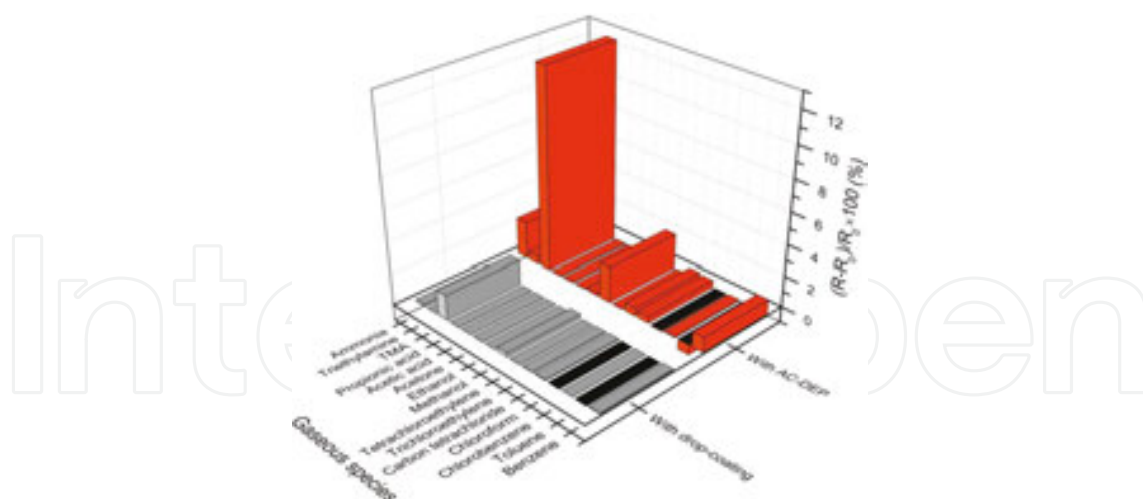


Figure 21. Selective response of the drop coated and AC-DEP assembled PEDOT/PSS-SWCNTs nanocomposite films to various vapours of 10 ppm. Reproduced from [193], with permission from Elsevier.

the sensing performances, for example good selectivity towards chloroform vapour over the other chlorinated methane vapour [192]. The targeted functionalization of CNTs by conducting polymer via electrochemical route is demonstrated to facilitate creation of high-density individually addressable nanosensor arrays, with improved sensitivity, detection limit and reproducibility [191].

It is also shown that oxygen plasma treatment of CNTs and their alignment in the nanocomposites film can improve the sensing performance in terms of sensitivity, selectivity, rapidity of response, good reversibility and stability [193]. Such effects are considered as manifestations of improved morphology and charge transport properties of thin film. For example, oxygen plasma functionalized and dielectrophoretically aligned CNTs-loaded PEDOT film-based sensors display (**Figure 21**) excellent responses for detection of 2–300 ppm NH_3 and 6–1000 ppb trimethylamine gases at room temperature. The presence of CNTs is conjugated polymer matrix is also known to improve sensitivity due to increase in degree of interactions during adsorption or desorption of the analyte [194]. For example, the sensitivity for NO_2 gas of polypyrrole–single-walled CNT nanocomposite is about ten times higher than that of pristine polypyrrole due to increase in the specific surface area by uniform polypyrrole coating on the single-wall CNTs. Nevertheless, though CNTs/polymer composites demonstrated to display improved sensing performance, the detailed sensing mechanism is still unclear, the cross-selectivity is poor and delayed recovery, stability and performance drift are the major issues to be resolved.

7. Conclusion and future directions

In conclusion, it is notable that CNTs-based polymer nanocomposites present an array of possibilities for their use in various technology developments. The electrical properties and dependent applications of CNTs-based nanocomposites (e.g. EMI shielding, antistatic) are

already satisfactory, though the scope for improvement cannot be ruled out especially in terms of cost reduction. In the context of thermal properties, CNTs-polymer nanocomposites with good thermal stability and appreciable thermal conductivity have already been exploited for heat sink and thermal-interfacing applications. However, for mechanical properties in particular, some key challenges need to be addressed and resolved so that the full potential of CNTs can be realized. Out of these challenges, the ability to acquire homogeneous dispersion of CNTs and their alignment in the polymer matrix remain major bottlenecks. The limitations faced due to this adversely affect the available filler surface area and thus the load transfer between the filler and the matrix leading to a compromise in terms of mechanical properties. With the increased understanding of functionalization chemistry in the recent years, the issue of dispersion has been partly circumvented. However, to compete with the existing carbon fibre-based nanocomposites, further efforts are needed in this direction. Novel functionalization routes are needed which enable maximum possible homogeneity in CNTs dispersion with least sacrifice on the part of mechanical properties of nanocomposites. Due to the large costs involved in the synthesis and processing of these nanocomposites, their commercial viability also needs mention in terms of key challenges. Furthermore, the high thermal conductivity of CNTs can be capitalized only when the high interfacial thermal resistance of nanotube networks can be minimized. In a nutshell, the future of CNTs-based polymer nanocomposites decisively hinges on the success achieved in the address of these key challenges.

Author details

Waseem Khan, Rahul Sharma and Parveen Saini*

*Address all correspondence to: pksaini@nplindia.org; parveensaini580@gmail.com

Polymeric and Soft Materials Section, Materials Physics and Engineering Division, CSIR-National Physical Laboratory, New Delhi, India

References

- [1] Iijima, S. Helical microtubules of graphitic carbon. *Nature* 354, 56–58 (1991).
- [2] Sinha, S., Barjami, S., Iannacchione, G., Schwab, A. & Muench, G. Off-axis Thermal Properties of Carbon Nanotube Films. *J. Nanoparticle Res.* 7, 651–657 (2005).
- [3] Hong, S. & Myung, S. Nanotube Electronics: A flexible approach to mobility. *Nat. Nanotechnol.* 2, 207–208 (2007).
- [4] Zeng, Y. *et al.* Enhanced adsorption of malachite green onto carbon nanotube/polyaniline composites. *J. Appl. Polym. Sci.* 127, 2475–2482 (2013).

- [5] Shao, D. *et al.* Polyaniline Multiwalled Carbon Nanotube Magnetic Composite Prepared by Plasma-Induced Graft Technique and Its Application for Removal of Aniline and Phenol. *J. Phys. Chem. C* 114, 21524–21530 (2010).
- [6] Ravindran, S., Chaudhary, S., Colburn, B., Ozkan, M. & Ozkan, C. S. Covalent Coupling of Quantum Dots to Multiwalled Carbon Nanotubes for Electronic Device Applications. *Nano Lett.* 3, 447–453 (2003).
- [7] Novak, J. P. *et al.* Nerve agent detection using networks of single-walled carbon nanotubes. *Appl. Phys. Lett.* 83, 4026 (2003).
- [8] Niyogi, S. *et al.* Chemistry of Single-Walled Carbon Nanotubes. *Accounts Chem. Res.* 35, 1105–1113 (2002).
- [9] Li, J. *et al.* Carbon Nanotube Sensors for Gas and Organic Vapor Detection. *Nano Lett.* 3, 929–933 (2003).
- [10] Kardimi, K. *et al.* Synthesis and characterization of carbon nanotubes decorated with Pt and PtRu nanoparticles and assessment of their electrocatalytic performance. *Int. J. Hydrog. Energy* 37, 1243–1253 (2012).
- [11] Bryning, M. B. *et al.* Carbon Nanotube Aerogels. *Adv. Mater.* 19, 661–664 (2007).
- [12] Bekyarova, E. *et al.* Chemically Functionalized Single-Walled Carbon Nanotubes as Ammonia Sensors †. *J. Phys. Chem. B* 108, 19717–19720 (2004).
- [13] Saini, P. in *Fundamentals of Conjugated Polymer Blends, Copolymers and Composites* (ed. Saini, P.) 449–518 (John Wiley & Sons, Inc., 2015). at <<http://doi.wiley.com/10.1002/9781119137160.ch9>>
- [14] Saini, P. in *Thermoset Nanocomposites* (ed. Mittal, V.) 211–237 (Wiley-VCH Verlag GmbH & Co. KGaA, 2013). at <<http://doi.wiley.com/10.1002/9783527659647.ch10>>
- [15] Xia, Z. *et al.* Direct observation of toughening mechanisms in carbon nanotube ceramic matrix composites. *Acta Mater.* 52, 931–944 (2004).
- [16] Flahaut, E. *et al.* Carbon nanotube-metal-oxide nanocomposites: microstructure, electrical conductivity and mechanical properties. *Acta Mater.* 48, 3803–3812 (2000).
- [17] Li, Q., Viereckl, A., Rottmair, C. A. & Singer, R. F. Improved processing of carbon nanotube/magnesium alloy composites. *Compos. Sci. Technol.* 69, 1193–1199 (2009).
- [18] Johnson, R. R., Johnson, A. T. C. & Klein, M. L. Probing the Structure of DNA-Carbon Nanotube Hybrids with Molecular Dynamics. *Nano Lett.* 8, 69–75 (2008).
- [19] Peng, C., Zhang, S., Jewell, D. & Chen, G. Z. Carbon nanotube and conducting polymer composites for supercapacitors. *Prog. Nat. Sci.* 18, 777–788 (2008).
- [20] Thostenson, E., Li, C. & Chou, T. Nanocomposites in context. *Compos. Sci. Technol.* 65, 491–516 (2005).

- [21] Saini, P. & Aror, M. in *New Polymers for Special Applications* (ed. De Souza Gomes, A.) (InTech, 2012). at <<http://www.intechopen.com/books/new-polymers-for-special-applications/microwave-absorption-and-emi-shielding-behavior-of-nanocomposites-based-on-intrinsically-conducting->>
- [22] Meincke, O. *et al.* Mechanical properties and electrical conductivity of carbon-nanotube filled polyamide-6 and its blends with acrylonitrile/butadiene/styrene. *Polymer* 45, 739–748 (2004).
- [23] Saini, P., Choudhary, V., Singh, B. P., Mathur, R. B. & Dhawan, S. K. Enhanced microwave absorption behavior of polyaniline-CNT/polystyrene blend in 12.4-18.0GHz range. *Synth. Met.* 161, 1522–1526 (2011).
- [24] Cai, L., Tabata, H. & Kawai, T. Self-assembled DNA networks and their electrical conductivity. *Appl. Phys. Lett.* 77, 3105 (2000).
- [25] Hersam, M. C., Hoole, A. C. F., O'Shea, S. J. & Welland, M. E. Potentiometry and repair of electrically stressed nanowires using atomic force microscopy. *Appl. Phys. Lett.* 72, 915 (1998).
- [26] Moniruzzaman, M. & Winey, K. I. Polymer Nanocomposites Containing Carbon Nanotubes. *Macromolecules* 39, 5194–5205 (2006).
- [27] Ma, P.-C., Siddiqui, N. A., Marom, G. & Kim, J.-K. Dispersion and functionalization of carbon nanotubes for polymer-based nanocomposites: A review. *Compos. Part Appl. Sci. Manuf.* 41, 1345–1367 (2010).
- [28] Liu, Y. & Kumar, S. Polymer/Carbon Nanotube Nano Composite Fibers-A Review. *Acs Appl. Mater. Interfaces* 6, 6069–6087 (2014).
- [29] Saito, Y., Dresselhaus, G. & Dresselhaus, M. S. *Physical properties of carbon nanotubes*. (London and Imperial College Press, 1998).
- [30] Dresselhaus, M. S., Dresselhaus, G. & Avouris, P. *Carbon Nanotubes: synthesis and structure and properties and applications*. (Berlin Springer-Verlag, 2001).
- [31] Meunier, V. & Lambin, P. Scanning tunneling microscopy and spectroscopy of topological defects in carbon nanotubes. *Carbon* 38, 1729–1733 (2000).
- [32] Charlier, J.-C., Ebbesen, T. W. & Lambin, P. Structural and electronic properties of pentagon-heptagon pair defects in carbon nanotubes. *Phys. Rev. B* 53, 11108–11113 (1996).
- [33] Lambin, P., Márk, G. I. & Biró, L. P. Structural and electronic properties of coiled and curled carbon nanotubes having a large number of pentagon-heptagon pairs. *Phys. Rev. B* 67, (2003).
- [34] Miyamoto, Y., Rubio, A., Berber, S., Yoon, M. & Tománek, D. Spectroscopic characterization of Stone-Wales defects in nanotubes. *Phys. Rev. B* 69, (2004).

- [35] Kim, P., Odom, T. W., Huang, J.-L. & Lieber, C. M. Electronic Density of States of Atomically Resolved Single-Walled Carbon Nanotubes: Van Hove Singularities and End States. *Phys. Rev. Lett.* 82, 1225–1228 (1999).
- [36] Ouyang, M., Huang, J. L., Cheung, C. L. & Lieber, C. M. Atomically resolved single-walled carbon nanotube intramolecular junctions. *Science* 291, 97 (2001).
- [37] Kim, H. *et al.* Scanning Tunneling Spectroscopy of a Semiconducting Heterojunction Nanotube on the Au(111) Surface. *Surf Sci* 581, 241 (2005).
- [38] Kim, H. *et al.* Direct Observation of Localized Defect States in Semiconductor Nanotube Junctions. *Phys. Rev. Lett.* 90, (2003).
- [39] Ishigami, M. *et al.* Identifying Defects in Nanoscale Materials. *Phys. Rev. Lett.* 93, (2004).
- [40] Carroll, D. L. *et al.* Electronic Structure and Localized States at Carbon Nanotube Tips. *Phys. Rev. Lett.* 78, 2811–2814 (1997).
- [41] Dean, K. A. & Chalamala, B. R. Experimental studies of the cap structure of single-walled carbon nanotubes. *J. Vac. Sci. Technol. B Microelectron. Nanometer Struct.* 21, 868 (2003).
- [42] Krätschmer, W., Lamb, L. D., Fostiropoulos, K. & Huffman, D. R. Solid C₆₀: a new form of carbon. *Nature* 347, 354–358 (1990).
- [43] Allouche, H. *et al.* Physical characteristics of the graphite electrode electric- arc as parameters for the formation of single-wall carbon nanotubes. in 1053–1054 (2000).
- [44] Razafinimanana, M. *et al.* Influence of doped graphite electrode in electric arc for the formation of single wall carbon nanotubes. in 649–654
- [45] Pacheco, M., Allouche, H., Monthieux, M., Razafinimanana, A. & Gleizes, A. Correlation between the plasma characteristics and the morphology and structure of the carbon phases synthesised by electric arc discharge. in (2001).
- [46] Kroto, H. W., Heath, J. R., O'Brien, S. C., Curl, R. F. & Smalley, R. E. C₆₀: Buckminsterfullerene. *Nature* 318, 162–163 (1985).
- [47] Guo, T. *et al.* Self-Assembly of Tubular Fullerenes. *J. Phys. Chem.* 99, 10694–10697 (1995).
- [48] Baker, R. T. K. Catalytic growth of carbon filaments. *Carbon* 27, 315–323 (1989).
- [49] Endo, M. *et al.* The production and structure of pyrolytic carbon nanotubes (PCNTs). *J. Phys. Chem. Solids* 54, 1841–1848 (1993).
- [50] Dai, H. *et al.* Single-wall nanotubes produced by metal-catalyzed disproportionation of carbon monoxide. *Chem. Phys. Lett.* 260, 471–475 (1996).
- [51] Dai, H., Wong, E. W. & Lieber, C. M. Probing Electrical Transport in Nanomaterials: Conductivity of Individual Carbon Nanotubes. *Science* 272, 523–526 (1996).

- [52] Odom, T. W., Huang, J. L., Kim, P. & Lieber, C. M. Atomic structure and electronic properties of single-walled carbonnanotubes. *Nature* 391, 62–64 (1998).
- [53] Ouyang, M. Energy Gaps in ‘Metallic’ Single-Walled Carbon Nanotubes. *Science* 292, 702–705 (2001).
- [54] Charlier, J.-C., Blase, X. & Roche, S. Electronic and transport properties of nanotubes. *Rev. Mod. Phys.* 79, 677–732 (2007).
- [55] Hone, J., Whitney, M., Piskoti, C. & Zettl, A. Thermal conductivity of single-walled carbon nanotubes. *Phys. Rev. B* 59, R2514-R2516 (1999).
- [56] Hone, J. *et al.* Electrical and thermal transport properties of magnetically aligned single wall carbon nanotube films. *Appl. Phys. Lett.* 77, 666 (2000).
- [57] Berber, S., Kwon, Y.-K. & Tománek, D. Unusually High Thermal Conductivity of Carbon Nanotubes. *Phys. Rev. Lett.* 84, 4613–4616 (2000).
- [58] Che, J., Çağın, T. & Goddard III, W. A. Thermal conductivity of carbon nanotubes. *Nanotechnology* 11, 65–69 (2000).
- [59] Pop, E., Mann, D., Wang, Q., Goodson, K. & Dai, H. Thermal Conductance of an Individual Single-Wall Carbon Nanotube above Room Temperature. *Nano Lett.* 6, 96–100 (2006).
- [60] Yakobson, B. I. & Avouris, P. Mechanical Properties of Carbon Nanotubes. *Top. Appl Phys* 80, 287–327 (2001).
- [61] Qian, D., Wagner, G. J., Liu, W. K., Yu, M.-F. & Ruoff, R. S. Mechanics of carbon nanotubes. *Appl. Mech. Rev.* 55, 495 (2002).
- [62] Reich, S., Thomsen, C. & Maultzsch, J. *Carbon Nanotubes: Basic Concepts and Physical Properties.* (New York: Wiley-VCH, 2004).
- [63] Yu, M. Strength and Breaking Mechanism of Multiwalled Carbon Nanotubes Under Tensile Load. *Science* 287, 637–640 (2000).
- [64] Ruoff, R. S., Tersoff, J., Lorents, D. C., Subramoney, S. & Chan, B. Radial deformation of carbon nanotubes by van der Waals forces. *Nature* 364, 514–516 (1993).
- [65] Yang, Y. H. & Li, W. Z. Radial elasticity of single-walled carbon nanotube measured by atomic force microscopy. *Appl. Phys. Lett.* 98, 041901 (2011).
- [66] Yu, M.-F., Kowalewski, T. & Ruoff, R. S. Investigation of the Radial Deformability of Individual Carbon Nanotubes under Controlled Indentation Force. *Phys. Rev. Lett.* 85, 1456–1459 (2000).
- [67] Kuryliszyn-Kudelska, I., Małolepszy, A., Mazurkiewicz, M., Stobinski, L. & Dobrowolski, W. Magnetic Properties of ‘As-Prepared’ and Chemically Modified Multiwalled Carbon Nanotubes. *Acta Phys. Pol.* 119, 597–599 (2011).

- [68] Maheshwari, P. H., Singh, R. & Mathur, R. B. Effect of heat treatment on the structure and stability of multiwalled carbon nanotubes produced by catalytic chemical vapor deposition technique. *Mater. Chem. Phys.* 134, 412–416 (2012).
- [69] Gupta, V. & Kotnala, R. K. Multifunctional Ferromagnetic Carbon-Nanotube Arrays Prepared by Pulse-Injection Chemical Vapor Deposition. *Angew. Chem. Int. Ed.* 51, 2916–2919 (2012).
- [70] Walters, D. A. *et al.* In-plane-aligned membranes of carbon nanotubes. *Chem. Phys. Lett.* 338, 14–20 (2001).
- [71] Kim, H. M. *et al.* Electrical conductivity and electromagnetic interference shielding of multiwalled carbon nanotube composites containing Fe catalyst. *Appl. Phys. Lett.* 84, 589 (2004).
- [72] Bahr, J. L., Mickelson, E. T., Bronikowski, M. J., Smalley, R. E. & Tour, J. M. Dissolution of small diameter single-wall carbon nanotubes in organic solvents? *Chem. Commun.* 193–194 (2001). doi:10.1039/b008042j
- [73] Hirsch, A. Functionalization of single-walled carbon nanotubes. *Angew Chem Int Ed* 41, 1853–1859 (2002).
- [74] Rinzler, A. G. *et al.* Large-scale purification of single-wall carbon nanotubes: process, product, and characterization. *Appl. Phys. Mater. Sci. Process.* 67, 29–37 (1998).
- [75] Liu, J. *et al.* Fullerene pipes. *Science* 280, 1253 (1998).
- [76] Holzinger, M. Functionalization of single-walled carbon nanotubes. (University Erlangen-Nürnberg, 2002).
- [77] Riggs, J. E., Guo, Z., Carroll, D. L. & Sun, Y.-P. Strong Luminescence of Solubilized Carbon Nanotubes. *J. Am. Chem. Soc.* 122, 5879–5880 (2000).
- [78] Lim, J. K. *et al.* Selective thiolation of single-walled carbon nanotubes. *Synth. Met.* 139, 521–527 (2003).
- [79] Nakajima, T., Kasamatsu, S. & Matsuo, Y. Synthesis and characterization of fluorinated carbon nanotubes. *Eur J Solid State Inorg Chem* 33, 831 (1996).
- [80] Unger, E., Graham, A., Kreupl, F., Liebau, M. & Hoenlein, W. Electrochemical functionalization of multi-walled carbon nanotubes for solvation and purification. *Curr. Appl. Phys.* 2, 107–111 (2002).
- [81] Chen, Y. K. *et al.* Purification and opening of carbon nanotubes via bromination. *Adv. Mater.* 8, 1012–1015 (1996).
- [82] Owens, F. J. & Iqbal, Z. Electrochemical functionalization of carbon nanotubes with hydrogen. in (2002).

- [83] Holzinger, M. *et al.* Sidewall Functionalization of Carbon Nanotubes This work was supported by the European Union under the 5th Framework Research Training Network 1999, HPRNT 1999-00011 FUNCARS. *Angew. Chem. Int. Ed.* 40, 4002 (2001).
- [84] Coleman, K. S., Bailey, S. R., Fogden, S. & Green, M. L. H. Functionalization of Single-Walled Carbon Nanotubes via the Bingel Reaction. *J. Am. Chem. Soc.* 125, 8722–8723 (2003).
- [85] Georgakilas, V. *et al.* Organic Functionalization of Carbon Nanotubes. *J. Am. Chem. Soc.* 124, 760–761 (2002).
- [86] Cui, Burghard, M. & Kern, K. Reversible Sidewall Osmylation of Individual Carbon Nanotubes. *Nano Lett.* 3, 613–615 (2003).
- [87] Lu, X., Tian, F., Wang, N. & Zhang, Q. Organic Functionalization of the Sidewalls of Carbon Nanotubes by Diels-Alder Reactions: A Theoretical Prediction. *Org. Lett.* 4, 4313–4315 (2002).
- [88] Bahr, J. L. *et al.* Functionalization of Carbon Nanotubes by Electrochemical Reduction of Aryl Diazonium Salts: A Bucky Paper Electrode. *J. Am. Chem. Soc.* 123, 6536–6542 (2001).
- [89] Kooi, S. E., Schlecht, U., Burghard, M. & Kern, K. Electrochemical Modification of Single Carbon Nanotubes. *Angew. Chem. Int. Ed.* 41, 1353–1355 (2002).
- [90] Bandow, S. *et al.* Purification of Single-Wall Carbon Nanotubes by Microfiltration. *J. Phys. Chem. B* 101, 8839–8842 (1997).
- [91] Duesberg, G. S., Burghard, M., Muster, J. & Philipp, G. Separation of carbon nanotubes by size exclusion chromatography. *Chem. Commun.* 435–436 (1998). doi:10.1039/a707465d
- [92] Krstic, V., Duesberg, G. S., Muster, J., Burghard, M. & Roth, S. Langmuir-Blodgett Films of Matrix-Diluted Single-Walled Carbon Nanotubes. *Chem. Mater.* 10, 2338–2340 (1998).
- [93] O'Connell, M. J. *et al.* Reversible water-solubilization of single-walled carbon nanotubes by polymer wrapping. *Chem. Phys. Lett.* 342, 265–271 (2001).
- [94] Smith, B. W. & Luzzi, D. E. Formation mechanism of fullerene peapods and coaxial tubes: a path to large scale synthesis. *Chem. Phys. Lett.* 321, 169–174 (2000).
- [95] Smith, B. W., Monthieux, M. & Luzzi, D. E. Carbon nanotube encapsulated fullerenes: a unique class of hybrid materials. *Chem. Phys. Lett.* 315, 31–36 (1999).
- [96] Jeon, I.-Y., Wook, D., Ashok, N. & Baek, J.-B. in *Carbon Nanotubes - Polymer Nanocomposites* (ed. Yellampalli, S.) (InTech, 2011). at <<http://www.intechopen.com/books/carbon-nanotubes-polymer-nanocomposites/functionalization-of-carbon-nanotubes>>

- [97] Saini, P., Choudhary, V., Singh, B. P., Mathur, R. B. & Dhawan, S. K. Polyaniline-MWCNT nanocomposites for microwave absorption and EMI shielding. *Mater. Chem. Phys.* 113, 919–926 (2009).
- [98] A chemical sensor for chloromethanes using a nanocomposite of multiwalled carbon nanotubes with poly(3-methylthiophene). *Sensors Actuators B Chem.* 106, 766–771 (2005).
- [99] Kar, P., Choudhury, A. & Verma, S. K. in *Fundamentals of Conjugated Polymer Blends, Copolymers and Composites* (ed. Saini, P.) 619–686 (John Wiley & Sons, Inc., 2015). at <<http://doi.wiley.com/10.1002/9781119137160.ch12>>
- [100] Rud, J. A., Lovell, L. S., Senn, J. W., Qiao, Q. & Mcleskey, J. T. Water soluble polymer/carbon nanotube bulk heterojunction solar cells. *J. Mater. Sci.* 40, 1455–1458 (2005).
- [101] Kanai, Y. & Grossman, J. C. Role of Semiconducting and Metallic Tubes in P3HT/Carbon-Nanotube Photovoltaic Heterojunctions: Density Functional Theory Calculations. *Nano Lett.* 8, 908–912 (2008).
- [102] Zhu, Z., Wang, G., Sun, M., Li, X. & Li, C. Fabrication and electrochemical characterization of polyaniline nanorods modified with sulfonated carbon nanotubes for supercapacitor applications. *Electrochimica Acta* 56, 1366–1372 (2011).
- [103] Liu, P. in *Fundamentals of Conjugated Polymer Blends, Copolymers and Composites* (ed. Saini, P.) 419–447 (John Wiley & Sons, Inc., 2015). at <<http://doi.wiley.com/10.1002/9781119137160.ch8>>
- [104] Yu, C., Kim, Y. S., Kim, D. & Grunlan, J. C. Thermoelectric Behavior of Segregated-Network Polymer Nanocomposites. *Nano Lett.* 9, 1283–1283 (2009).
- [105] Yao, Q., Chen, L., Zhang, W., Liufu, S. & Chen, X. Enhanced Thermoelectric Performance of Single-Walled Carbon Nanotubes/Polyaniline Hybrid Nanocomposites. *ACS Nano* 4, 2445–2451 (2010).
- [106] Saini, P. & Choudhary, V. Enhanced electromagnetic interference shielding effectiveness of polyaniline functionalized carbon nanotubes filled polystyrene composites. *J. Nanoparticle Res.* 15, (2013).
- [107] Daniel, I. M. *Engineering mechanics of composite materials*. (Oxford University Press, 2006).
- [108] Saini, P. in *Fundamentals of Conjugated Polymer Blends, Copolymers and Composites* (ed. Saini, P.) 1–118 (John Wiley & Sons, Inc., 2015). at <<http://doi.wiley.com/10.1002/9781119137160.ch1>>
- [109] Berrod, G., Vidal, A., Papirer, E. & Donnet, J. B. Reinforcement of siloxane elastomers by silica. Interactions between an oligomer of poly(dimethylsiloxane) and a fumed silica. *J. Appl. Polym. Sci.* 23, 2579–2590 (1979).
- [110] Johnson, B. L. *Industrial and Engineering Chemistry*. (1951).

- [111] Choudhary, V. & Gupt, A. in *Carbon Nanotubes - Polymer Nanocomposites* (ed. Yellampalli, S.) (InTech, 2011). at <<http://www.intechopen.com/books/carbon-nanotubes-polymer-nanocomposites/polymer-carbon-nanotube-nanocomposites>>
- [112] Choudhary, V., Singh, B. P. & Mathur, R. B. in *Syntheses and Applications of Carbon Nanotubes and Their Composites* (ed. Suzuki, S.) (InTech, 2013). at <<http://www.intechopen.com/books/syntheses-and-applications-of-carbon-nanotubes-and-their-composites/carbon-nanotubes-and-their-composites>>
- [113] Coleman, J. N., Khan, U., Blau, W. J. & Gun'ko, Y. K. Small but strong: A review of the mechanical properties of carbon nanotube-polymer composites. *Carbon* 44, 1624–1652 (2006).
- [114] Spitalsky, Z., Tasis, D., Papagelis, K. & Galiotis, C. Carbon nanotube-polymer composites: Chemistry, processing, mechanical and electrical properties. *Prog. Polym. Sci.* 35, 357–401 (2010).
- [115] Badaire, S., Poulin, P., Maugey, M. & Zakri, C. In Situ Measurements of Nanotube Dimensions in Suspensions by Depolarized Dynamic Light Scattering. *Langmuir* 20, 10367–10370 (2004).
- [116] Bandyopadhyaya, R., Nativ-Roth, E., Regev, O. & Yerushalmi-Rozen, R. Stabilization of Individual Carbon Nanotubes in Aqueous Solutions. *Nano Lett.* 2, 25–28 (2002).
- [117] Wu, H.-X. *et al.* Polymer-wrapped multiwalled carbon nanotubes synthesized via microwave-assisted in situ emulsion polymerization and their optical limiting properties. *Carbon* 45, 2866–2872 (2007).
- [118] Pei, X., Hu, L., Liu, W. & Hao, J. Synthesis of water-soluble carbon nanotubes via surface initiated redox polymerization and their tribological properties as water-based lubricant additive. *Eur. Polym. J.* 44, 2458–2464 (2008).
- [119] Cheng, F., Imin, P., Maunders, C., Botton, G. & Adronov, A. Soluble, Discrete Supramolecular Complexes of Single-Walled Carbon Nanotubes with Fluorene-Based Conjugated Polymers. *Macromolecules* 41, 2304–2308 (2008).
- [120] Bryning, M. B., Milkie, D. E., Islam, M. F., Kikkawa, J. M. & Yodh, A. G. Thermal conductivity and interfacial resistance in single-wall carbon nanotube epoxy composites. *Appl. Phys. Lett.* 87, 161909 (2005).
- [121] Lau, K., Lu, M., Cheung, H., Sheng, F. & Li, H. Thermal and mechanical properties of single-walled carbon nanotube bundle-reinforced epoxy nanocomposites: the role of solvent for nanotube dispersion. *Compos. Sci. Technol.* 65, 719–725 (2005).
- [122] De la Chapelle, M. L. *et al.* Raman characterization of singlewalled carbon nanotubes and PMMA-nanotubes composites. *Synth. Met.* 103, 2510–2512 (1999).
- [123] Du, F., Fischer, J. E. & Winey, K. I. Coagulation method for preparing single-walled carbon nanotube/poly(methyl methacrylate) composites and their modulus, electrical

- conductivity, and thermal stability. *J. Polym. Sci. Part B Polym. Phys.* 41, 3333–3338 (2003).
- [124] Barrau, S. *et al.* Effect of Palmitic Acid on the Electrical Conductivity of Carbon Nanotubes-Epoxy Resin Composites. *Macromolecules* 36, 9678–9680 (2003).
- [125] Islam, M. F., Rojas, E., Bergey, D. M., Johnson, A. T. & Yodh, A. G. High Weight Fraction Surfactant Solubilization of Single-Wall Carbon Nanotubes in Water. *Nano Lett.* 3, 269–273 (2003).
- [126] Benoit, J.-M. *et al.* Transport properties of PMMA-Carbon Nanotubes composites. *Synth. Met.* 121, 1215–1216 (2001).
- [127] Dalton, A. B. *et al.* Super-tough carbon-nanotube fibres. *Nature* 423, 703–703 (2003).
- [128] Verma, P., Saini, P. & Choudhary, V. Designing of carbon nanotube/polymer composites using melt recirculation approach: Effect of aspect ratio on mechanical, electrical and EMI shielding response. *Mater. Des.* 88, 269–277 (2015).
- [129] Verma, P., Saini, P., Malik, R. S. & Choudhary, V. Excellent electromagnetic interference shielding and mechanical properties of high loading carbon-nanotubes/polymer composites designed using melt recirculation equipped twin-screw extruder. *Carbon* 89, 308–317 (2015).
- [130] Andrews, R., Jacques, D., Qian, D. & Rantell, T. Multiwall Carbon Nanotubes: Synthesis and Application. *Accounts Chem. Res.* 35, 1008–1017 (2002).
- [131] Bhattacharyya, A. R. *et al.* Crystallization and orientation studies in polypropylene/single wall carbon nanotube composite. *Polymer* 44, 2373–2377 (2003).
- [132] Tang, W., Santare, M. H. & Advani, S. G. Melt processing and mechanical property characterization of multi-walled carbon nanotube/high density polyethylene (MWNT/HDPE) composite films. *Carbon* 41, 2779–2785 (2003).
- [133] Haggenueller, R., Gommans, H. H., Rinzler, A. G., Fischer, J. E. & Winey, K. I. Aligned single-wall carbon nanotubes in composites by melt processing methods. *Chem. Phys. Lett.* 330, 219–225 (2000).
- [134] Vigolo, B. Macroscopic Fibers and Ribbons of Oriented Carbon Nanotubes. *Science* 290, 1331–1334 (2000).
- [135] Xia, H., Wang, Q., Li, K. & Hu, G.-H. Preparation of polypropylene/carbon nanotube composite powder with a solid-state mechanochemical pulverization process. *J. Appl. Polym. Sci.* 93, 378–386 (2004).
- [136] Dhand, C. *et al.* Preparation of polyaniline/multiwalled carbon nanotube composite by novel electrophoretic route. *Carbon* 46, 1727–1735 (2008).
- [137] Regev, O., ElKati, P. N. B., Loos, J. & Koning, C. E. Preparation of Conductive Nanotube-Polymer Composites Using Latex Technology. *Adv. Mater.* 16, 248–251 (2004).

- [138] Ramasubramaniam, R., Chen, J. & Liu, H. Homogeneous carbon nanotube/polymer composites for electrical applications. *Appl. Phys. Lett.* 83, 2928 (2003).
- [139] Baughman, R. H. Carbon Nanotubes--the Route Toward Applications. *Science* 297, 787–792 (2002).
- [140] Bryning, M. B., Islam, M. F., Kikkawa, J. M. & Yodh, A. G. Very Low Conductivity Threshold in Bulk Isotropic Single-Walled Carbon Nanotube-Epoxy Composites. *Adv. Mater.* 17, 1186–1191 (2005).
- [141] Sandler, J. K. W., Kirk, J. E., Kinloch, I. A., Shaffer, M. S. P. & Windle, A. H. Ultra-low electrical percolation threshold in carbon-nanotube-epoxy composites. *Polymer* 44, 5893–5899 (2003).
- [142] Du, F., Fischer, J. E. & Winey, K. I. Effect of nanotube alignment on percolation conductivity in carbon nanotube/polymer composites. *Phys. Rev. B* 72, (2005).
- [143] Bai, J. B. & Allaoui, A. Effect of the length and the aggregate size of MWNTs on the improvement efficiency of the mechanical and electrical properties of nanocomposites-experimental investigation. *Compos. Part Appl. Sci. Manuf.* 34, 689–694 (2003).
- [144] Li, X. *et al.* Fabrication and characterization of well-dispersed single-walled carbon nanotube/polyaniline composites. *Carbon* 41, 1670–1673 (2003).
- [145] Ramanathan, T., Liu, H. & Brinson, L. C. Functionalized SWNT/polymer nanocomposites for dramatic property improvement. *J. Polym. Sci. Part B Polym. Phys.* 43, 2269–2279 (2005).
- [146] Valentini, L., Armentano, I., Puglia, D. & Kenny, J. M. Dynamics of amine functionalized nanotubes/epoxy composites by dielectric relaxation spectroscopy. *Carbon* 42, 323–329 (2004).
- [147] Tamburri, E. *et al.* Modulation of electrical properties in single-walled carbon nanotube/conducting polymer composites. *Carbon* 43, 1213–1221 (2005).
- [148] Yuen, S.-M. *et al.* Silane-modified MWCNT/PMMA composites - Preparation, electrical resistivity, thermal conductivity and thermal stability. *Compos. Part Appl. Sci. Manuf.* 38, 2527–2535 (2007).
- [149] Gojny, F. H. *et al.* Evaluation and identification of electrical and thermal conduction mechanisms in carbon nanotube/epoxy composites. *Polymer* 47, 2036–2045 (2006).
- [150] Biercuk, M. J. *et al.* Carbon nanotube composites for thermal management. *Appl. Phys. Lett.* 80, 2767 (2002).
- [151] Evseeva, L. E. & Tanaeva, S. A. Thermal conductivity of micro-and nanostructural epoxy composites at low temperatures. *Mech. Compos. Mater.* 44, 87–92 (2008).
- [152] Guthy, C., Du, F., Brand, S., Winey, K. I. & Fischer, J. E. Thermal Conductivity of Single-Walled Carbon Nanotube/PMMA Nanocomposites. *J. Heat Transf.* 129, 1096 (2007).

- [153] Velasco-Santos, C., Martínez-Hernández, A. L., Fisher, F. T., Ruoff, R. & Castaño, V. M. Improvement of Thermal and Mechanical Properties of Carbon Nanotube Composites through Chemical Functionalization. *Chem. Mater.* 15, 4470–4475 (2003).
- [154] Choi, E. S. *et al.* Enhancement of thermal and electrical properties of carbon nanotube polymer composites by magnetic field processing. *J. Appl. Phys.* 94, 6034 (2003).
- [155] Du, F., Guthy, C., Kashiwagi, T., Fischer, J. E. & Winey, K. I. An infiltration method for preparing single-wall nanotube/epoxy composites with improved thermal conductivity. *J. Polym. Sci. Part B Polym. Phys.* 44, 1513–1519 (2006).
- [156] at <http://science.nasa.gov/science-news/science-at-nasa/2005/27jul_nanotech/>
- [157] Gao, J. *et al.* Continuous Spinning of a Single-Walled Carbon Nanotube-Nylon Composite Fiber. *J. Am. Chem. Soc.* 127, 3847–3854 (2005).
- [158] Zabihi, O., Ahmadi, M., Akhlaghi bagherjeri, M. & Naebe, M. One-pot synthesis of aminated multi-walled carbon nanotube using thiol-ene click chemistry for improvement of epoxy nanocomposites properties. *Rsc Adv* 5, 98692–98699 (2015).
- [159] Ji, J. *et al.* Significant Improvement of Mechanical Properties Observed in Highly Aligned Carbon-Nanotube-Reinforced Nanofibers. *J. Phys. Chem. C* 113, 4779–4785 (2009).
- [160] Liao, K. & Li, S. Interfacial characteristics of a carbon nanotube-polystyrene composite system. *Appl. Phys. Lett.* 79, 4225 (2001).
- [161] Huang, Y. *et al.* The influence of single-walled carbon nanotube structure on the electromagnetic interference shielding efficiency of its epoxy composites. *Carbon* 45, 1614–1621 (2007).
- [162] Krishnamoorti, R. & Giannelis, E. P. Rheology of End-Tethered Polymer Layered Silicate Nanocomposites. *Macromolecules* 30, 4097–4102 (1997).
- [163] Mitchell, C. A., Bahr, J. L., Arepalli, S., Tour, J. M. & Krishnamoorti, R. Dispersion of Functionalized Carbon Nanotubes in Polystyrene. *Macromolecules* 35, 8825–8830 (2002).
- [164] Pötschke, P., Abdel-Goad, M., Alig, I., Dudkin, S. & Lellinger, D. Rheological and dielectrical characterization of melt mixed polycarbonate-multiwalled carbon nanotube composites. *Polymer* 45, 8863–8870 (2004).
- [165] Yang, Y., Gupta, M. C., Dudley, K. L. & Lawrence, R. W. Novel Carbon Nanotube-Polystyrene Foam Composites for Electromagnetic Interference Shielding. *Nano Lett.* 5, 2131–2134 (2005).
- [166] Li, N. *et al.* Electromagnetic Interference (EMI) Shielding of Single-Walled Carbon Nanotube Epoxy Composites. *Nano Lett.* 6, 1141–1145 (2006).
- [167] Zhang, L. L., Zhou, R. & Zhao, X. S. Graphene-based materials as supercapacitor electrodes. *J. Mater. Chem.* 20, 5983 (2010).

- [168] Wang, G., Zhang, L. & Zhang, J. A review of electrode materials for electrochemical supercapacitors. *Chem Soc Rev* 41, 797–828 (2012).
- [169] Zhang, L. L. & Zhao, X. S. Carbon-based materials as supercapacitor electrodes. *Chem. Soc. Rev.* 38, 2520 (2009).
- [170] Fu, Q. *et al.* Novel non-covalent sulfonated multiwalled carbon nanotubes from p-toluenesulfonic acid/glucose doped polypyrrole for electrochemical capacitors. *Synth. Met.* 161, 373–378 (2011).
- [171] Frackowiak, E., Khomenko, V., Jurewicz, K., Lota, K. & Béguin, F. Supercapacitors based on conducting polymers/nanotubes composites. *J. Power Sources* 153, 413–418 (2006).
- [172] Fang, Y. *et al.* Self-supported supercapacitor membranes: Polypyrrole-coated carbon nanotube networks enabled by pulsed electrodeposition. *J. Power Sources* 195, 674–679 (2010).
- [173] Oh, J. *et al.* Preparation and electrochemical characterization of porous SWNT-PPy nanocomposite sheets for supercapacitor applications. *Synth. Met.* 158, 638–641 (2008).
- [174] Ren, S. *et al.* Toward Efficient Carbon Nanotube/P3HT Solar Cells: Active Layer Morphology, Electrical, and Optical Properties. *Nano Lett.* 11, 5316–5321 (2011).
- [175] Miller, A. J., Hatton, R. A. & Silva, S. R. P. Water-soluble multiwall-carbon-nanotube-polythiophene composite for bilayer photovoltaics. *Appl. Phys. Lett.* 89, 123115 (2006).
- [176] Geng, J. & Zeng, T. Influence of Single-Walled Carbon Nanotubes Induced Crystallinity Enhancement and Morphology Change on Polymer Photovoltaic Devices. *J. Am. Chem. Soc.* 128, 16827–16833 (2006).
- [177] Meng, C., Liu, C. & Fan, S. A Promising Approach to Enhanced Thermoelectric Properties Using Carbon Nanotube Networks. *Adv. Mater.* 22, 535–539 (2010).
- [178] Yu, C., Choi, K., Yin, L. & Grunlan, J. C. Light-Weight Flexible Carbon Nanotube Based Organic Composites with Large Thermoelectric Power Factors. *Acs Nano* 5, 7885–7892 (2011).
- [179] Kim, D., Kim, Y., Choi, K., Grunlan, J. C. & Yu, C. Improved Thermoelectric Behavior of Nanotube-Filled Polymer Composites with Poly(3,4-ethylenedioxythiophene) Poly(styrenesulfonate). *Acs Nano* 4, 513–523 (2010).
- [180] Yu, C., Kim, Y. S., Kim, D. & Grunlan, J. C. Thermoelectric Behavior of Segregated-Network Polymer Nanocomposites. *Nano Lett.* 8, 4428–4432 (2008).
- [181] Wang, Q., Yao, Q., Chang, J. & Chen, L. Enhanced thermoelectric properties of CNT/PANI composite nanofibers by highly orienting the arrangement of polymer chains. *J. Mater. Chem.* 22, 17612 (2012).

- [182] Hewitt, C. A. *et al.* Varying the concentration of single walled carbon nanotubes in thin film polymer composites, and its effect on thermoelectric power. *Appl. Phys. Lett.* 98, 183110 (2011).
- [183] Shawky, H. A., Chae, S.-R., Lin, S. & Wiesner, M. R. Synthesis and characterization of a carbon nanotube/polymer nanocomposite membrane for water treatment. *Desalination* 272, 46–50 (2011).
- [184] Liu, Y.-L., Chang, Y., Chang, Y.-H. & Shih, Y.-J. Preparation of Amphiphilic Polymer-Functionalized Carbon Nanotubes for Low-Protein-Adsorption Surfaces and Protein-Resistant Membranes. *Acs Appl. Mater. Interfaces* 2, 3642–3647 (2010).
- [185] Celik, E., Park, H., Choi, H. & Choi, H. Carbon nanotube blended polyethersulfone membranes for fouling control in water treatment. *Water Res.* 45, 274–282 (2011).
- [186] Qiu, S. *et al.* Preparation and properties of functionalized carbon nanotube/PSF blend ultrafiltration membranes. *J. Membr. Sci.* 342, 165–172 (2009).
- [187] Choi, J.-H., Jegal, J. & Kim, W.-N. Fabrication and characterization of multi-walled carbon nanotubes/polymer blend membranes. *J. Membr. Sci.* 284, 406–415 (2006).
- [188] Brunet, L. *et al.* Properties of Membranes Containing Semi-dispersed Carbon Nanotubes. *Environ. Eng. Sci.* 25, 565–576 (2008).
- [189] Hatchett, D. W. & Josowicz, M. Composites of Intrinsically Conducting Polymers as Sensing Nanomaterials. *Chem. Rev.* 108, 746–769 (2008).
- [190] Choi, H. H., Lee, J., Dong, K.-Y., Ju, B.-K. & Lee, W. Gas Sensing performance of composite materials using conducting polymer/single-walled carbon nanotubes. *Macromol. Res.* 20, 143–146 (2012).
- [191] Zhang, T., Nix, M. B., Yoo, B.-Y., Deshusses, M. A. & Myung, N. V. Electrochemically Functionalized Single-Walled Carbon Nanotube Gas Sensor. *Electroanalysis* 18, 1153–1158 (2006).
- [192] Kar, P. & Choudhury, A. Carboxylic acid functionalized multi-walled carbon nanotube doped polyaniline for chloroform sensors. *Sensors Actuators B Chem.* 183, 25–33 (2013).
- [193] Jian, J. *et al.* Gas-sensing characteristics of dielectrophoretically assembled composite film of oxygen plasma-treated SWCNTs and PEDOT/PSS polymer. *Sensors Actuators B Chem.* 178, 279–288 (2013).
- [194] An, K. H., Jeong, S. Y., Hwang, H. R. & Lee, Y. H. Enhanced Sensitivity of a Gas Sensor Incorporating Single-Walled Carbon Nanotube-Polypyrrole Nanocomposites. *Adv. Mater.* 16, 1005–1009 (2004).
- [195] Wang, F., Gu, H. & Swager, T. M. Carbon Nanotube/Polythiophene Chemiresistive Sensors for Chemical Warfare Agents. *J. Am. Chem. Soc.* 130, 5392–5393 (2008).

